Dynamical Climatology

Rossby adjustment over a step.

by

M.K. Davey, A.E. Gill, E.R. Johnson
and P.F. Linden

DCTN 34 January 1986

Meteorological Office (Met. O. 20)
London Road
Bracknell
Berkshire RG12 2SZ

DYNAMICAL CLIMATOLOGY TECHNICAL NOTE NO. 34

ROSSBY ADJUSTMENT OVER A STEP

by

M K Davey, A E Gill

Meteorological Office, Hooke Institute, Oxford

E R Johnson

Department of Mathematics, University College London

and

P F Linden

Department of Applied Mathematics and Theoretical Physics
University of Cambridge

Met O 20 (Dynamical
Climatology Branch)
Meteorological Office
London Road
Bracknell
Berkshire, U.K. RG12 2SZ

January 1986

Note: This paper has not been published. Permission to quote from it should be obtained from the Assistant Director of the above Meteorological Office Branch.

Rossby adjustment over a step

M.K. Davey*, A.E. Gill*, E.R.Johnson+
and P.F. Linden•

*Meteorological Office Unit
Hooke Institute for Atmospheric Research,
Clarendon Laboratory, Parks Road, Oxford OX1 3PU.

•Department of Applied Mathematics and Theoretical Physics,
University of Cambridge, Silver Street, Cambridge CB3 9EW.

+ Department of Mathematics, University College London,
Gower St., London WC1E 6BT.

Abstract

The adjustment of a rotating fluid to a geostrophic equilibrium is now a classical problem in the theory of rotating fluids and is associated with the name of Rossby because of his pioneering work in this subject. The case of particular interest here is the one where the fluid is initially at rest but has a discontinuity in surface elevation along a certain line. If the bottom is flat, the adjustment gives rise to a jet flowing along the line of the initial discontinuity, the width of the jet being the Rossby radius of deformation. This paper examines how the flow is modified when the bottom is not flat, but has a step-like

discontinuity running perpendicular to the line of the initial jump in surface elevation, giving rise to double Kelvin waves which propagate along the step.

The effect of adding a vertical coast perpendicular to the step is also considered. When the double Kelvin wave propagates offshore, it leaves behind a state with no transport across the step. With propagation toward the coast, however, there is pinching of the longshore current into a narrow boundary layer.

The problem is examined using (a) linear analysis, (b) laboratory experiments, and (c) numerical experiments.

1. Introduction

In 1937 and 1938, Rossby considered the mechanisms by which pressure and velocity distributions in the atmosphere and ocean undergo mutual adjustment towards a geostrophic equilibrium in which pressure gradients are balanced by the Coriolis acceleration. He illustrated the process by considering a flat bottomed shallow layer of fluid with an initial non-equilibrium distribution of surface elevation and velocity. A classical case is the one where the initial velocity (u,v) is zero but the surface elevation η has a discontinuity along a certain line x = o, i.e.

$$u = v = o, \quad \eta = \eta_o \operatorname{sgn} x \qquad \text{at } t = o. \tag{1.1}$$

where

$$\operatorname{sgn} x = \begin{cases} 1 & x > o \\ -1 & x < o \end{cases} \tag{1.2}$$

(We shall assume $\eta_o > o$ without loss of generality.) For small disturbances, the equations satisfied are the linear shallow water equations

$$u_t - fv = -g\,\eta_x, \tag{1.3}$$

$$v_t + fu = -g\,\eta_y, \tag{1.4}$$

$$\eta_t + (Hu)_x + (Hv)_y = o, \tag{1.5}$$

where f is the Coriolis parameter, g the acceleration due to (possibly reduced) gravity and H the undisturbed depth of the fluid. For convenience, we take f > o. In the classical case, H

is uniform over the whole domain and the result of the adjustment is a jet running along the line of the initial surface discontinuity, i.e. spread about the line $x = 0$. The problem is discussed fully in Chapter 7 of Gill (1982).

To understand the behaviour of the atmosphere and ocean, the adjustment of a stratified fluid over bottom topography needs to be considered. Some numerical experiments by Hsieh and Gill (1984) with quite simple configurations indicate that a rich variety of behaviour is possible, and these need to be explored in a systematic manner. Here we begin the process by considering a shallow homogeneous layer of fluid with simple step-like topography. A case with undisturbed depth H given by

$$H = \begin{cases} H_- & y < 0 \\ H_+ & y > 0 \end{cases} \qquad (1.6)$$

(see Fig. 1) is solved analytically in the next section, and gives rise to some very interesting behaviour. Results are illustrated using numerical integrations of the shallow-water equations in a similar geometry. Reduced gravity is used in the numerical experiments, so the deformation scale is the internal Rossby radius. (The shallow-water equations can in this sense be regarded as applying to the bottom layer of a system with a relatively deep overlying layer.)

The effect of adding a wall-like coast running perpendicular to the step is investigated next. Numerical experiments are described first, in section 3, followed by analytic solutions for steady cases in section 4. The coast acts as a barrier to double Kelvin waves propagating onshore, so behaviour for $H_- > H_+$ is very different from that with $H_- < H_+$. With $H_- > H_+$ the double Kelvin

waves carry coastal information far offshore: this phenomenon has been associated with flow along the Mendocino escarpment off central California (see Willmott 1984 for a two-layer model). For $H_- < H_+$ however, there is very little disturbance offshore, and longshore currents are concentrated into a narrow boundary layer near the intersection between the step and the coast.

In Section 5 we describe some laboratory experiments on geostrophic adjustment of a coastal current in the presence of step topography. A two-layer stratification is established in a rotating channel on both sides of a vertical barrier adjacent to one of the side walls of the channel. Different larger depths are used on the two sides, so that the density interface has an initial discontinuity in depth which is perpendicular to the step change in depth half-way along the channel. This reduced gravity adjustment corresponds closely with the numerical calculations described in Section 4.

It is observed that the coastal current is diverted perpendicular to the coast by the step. If the upper layer is approaching the shallower end, the double Kelvin wave propagates across the tank away from the coast (for $f > o$), and the current is diverted off-shore. On the other hand, when the upper layer is approaching deeper water, the topographic wave travels towards the coast and any transport across the step is confined to a thin boundary layer on the coast. Experiments were also carried out on currents in which there was no upper layer on the outer side of the barrier. In this case, the coastal current is bounded by a front and advection of fluid elements is important. This case, not treated by the theoretical calculations, exhibits the same features as the two-layer case.

2. Adjustment over a step

As Rossby showed, the solution of the problem is greatly facilitated by considering the potential vorticity equation. This is derived by first eliminating η from (1.3) and (1.4) to get the vorticity equation

$$\zeta_t + f(u_x + v_y) = 0, \tag{2.1}$$

where

$$\zeta = v_x - u_y. \tag{2.2}$$

Then the divergence is eliminated between (2.1) and (1.5) to give

$$\left[\frac{\eta}{H} - \frac{\zeta}{f}\right]_t + \frac{1}{H}\left[uH_x + vH_y\right] = 0. \tag{2.3}$$

The step topography has the great convenience that the bottom slope ∇H is non-zero only along the line $y = 0$ and is zero everywhere else. Thus (2.3) reduces to

$$\left[\frac{\eta}{H} - \frac{\zeta}{f}\right]_t = 0 \quad \text{except on } y = 0. \tag{2.4}$$

For the initial conditions (1.1), this can be integrated with respect to time to give

$$\frac{\eta}{H} - \frac{\zeta}{f} = \frac{\eta_0}{H} \operatorname{sgn} x \quad \text{except on } y = 0. \tag{2.5}$$

Furthermore, since for linearised motion particles move only an infinitesimal distance from their original position, the potential vorticity at any location remains the same for all times.

Consider first the adjustment for large y, i.e. far enough from the step for the motion not to be influenced by the step. The flow will take the classical form appropriate to a flat bottom, and in a time of the order of the inertial period will be close to the geostrophic equilibrium for which the velocity v and surface elevations are functions of x only. Thus (1.3) reduces to the geostrophic balance

$$fv = g\eta_x \tag{2.6}$$

and (2.5) becomes

$$\frac{\eta}{H} - \frac{v_x}{f} = \frac{\eta_o}{H} \operatorname{sgn} x. \tag{2.7}$$

These equations are easily solved to give

$$\eta = \eta_o \operatorname{sgn} x \, (1 - e^{-|x|/a}) \tag{2.8}$$

$$v = (gH)^{1/2} \frac{\eta_o}{H} e^{-|x|/a} \tag{2.9}$$

where

$$a = (gH)^{1/2}/f \tag{2.10}$$

is the Rossby deformation radius. With the sign convention that η_o is positive, the velocity v is positive.

We now ask whether the solutions on the two sides of the step are compatible. In particular, is the mass flux of the jet the same on the upstream and downstream sides of the step? The flux can be computed without reference to the detailed solution simply by integrating (2.6) with respect to x to give

$$f\int_{-\infty}^{\infty} v\,dx = 2g\eta_o. \qquad (2.11)$$

The volume flux is thus given by

$$H\int_{-\infty}^{\infty} v\,dx = 2gH\eta_o/f. \qquad (2.12)$$

Since H is different on the two sides of the step, the flux is different as well. Suppose $H_- < H_+$. Then the jet approaches the step from the shallow side $y < 0$ with a small flux and leaves the step on the deep side $y > 0$ with a large flux. Clearly something must happen at the step.

In the initial stage of adjustment, the fluid must seek to accommodate the discontinuity in flux at the step by sending out a disturbance from the origin, behind which there will be a flux away from the origin. The only available disturbance with this property would seem to be a double Kelvin wave which propagates along the topographic step with the deep water on its left for $f > 0$. (Longuet-Higgins 1968.) Thus the double Kelvin wave coming from the origin can only affect the region $x > 0$, and it is this property which gives the problem its intriguing asymmetry.

The structure of the double Kelvin wave is very similar to that given by (2.8) and (2.9), but the flow is now directed parallel to the topographic step and the surface elevation approaches η_o at both $y = +\infty$ and $y = -\infty$. The surface elevation is continuous across the step, so it must have the form

$$\eta = \eta_o - A e^{-|y|/a_\pm} \tag{2.13}$$

where

$$a_\pm = (gH_\pm)^{1/2}/f \quad . \tag{2.14}$$

is the Rossby radius determined by the local depth on either side of the step. It follows from the geostrophic relationship (see 1.4)

$$fu = -g\eta_y \tag{2.15}$$

that the along-step velocity is given by

$$u = \begin{cases} \frac{gA}{fa_-} e^{y/a_-} & y < o \\ \frac{-gA}{fa_+} e^{-y/a_+} & y > o \end{cases} \tag{2.16}$$

so the jet is discontinuous over the step. In fact (2.16) shows that the flow has opposite signs on the two sides of the step!

The variable A in (2.13) and (2.16) is a function of x and t. The equation it satisfies may be obtained by substituting (2.13) and (2.16) in (1.3) to find v, and then applying the

condition that the flux Hv is continuous at y = 0. The result is

$$(H_-^{1/2} + H_+^{1/2}) A_t + g^{1/2} (H_+ - H_-) A_x = 0, \qquad (2.17)$$

showing that the wave travels in the x direction at speed c given by

$$c = (gH_+)^{1/2} - (gH_-)^{1/2} \quad . \qquad (2.18)$$

However the details of the double Kelvin wave need not concern us here , apart from the fact that it travels along the step with deep water to its left and, after it has passed, leaves behind a flow of the form given by (2.13) and (2.16). All that is required now to give a consistent steady state is to choose A so that the fluxes match.

First there is a flux along the topographic step away from the origin in y < 0. By integrating (2.15) with respect to y, it follows that this flux is given by

$$H_- \int_{-\infty}^{\infty} u \, dy = H_- g A / f \quad . \qquad (2.19)$$

This matches the flux (2.12) toward the step provided

$$A = 2\eta_0 \quad . \qquad (2.20)$$

Similarly, the flux along the topographic step toward the origin is entirely in the region y > 0 and follows by integrating (2.15) to give, when the value of A is substituted from (2.20)

$$H_+ \int_{-\infty}^{\infty} u\,dy = -2gH_+\eta_0/f \qquad (2.21)$$

This exactly matches the flux (2.12) away from the step so giving a consistent final equilibrium state.

A sketch showing contours of surface elevation for the above solution is given in fig. 2. Details of how the jet turns when it reaches the step have not been calculated analytically, nor have the details at the double Kelvin wave front, so these are shown by broken lines. However, the picture that emerges is most intriguing. Firstly, in the final state, the topographic step acts as a complete barrier to the approaching jet, which is completely deflected along the step. The only flow across the step is in the Kelvin wave front, which becomes more and more remote from the path of the original jet as time progresses. The other remarkable property of the solution is the asymmetry. A jet approaching deeper water in the northern hemisphere is deflected to the right. The sign changes with f and a jet approaching shallow water is deflected the other way. Because of these interesting properties, it was decided to carry out laboratory and numerical experiments to further study the problem, and these are reported below.

Numerical results with no wall

To illustrate the variety of possible behaviour for flow over a step, the linear shallow-water equations (1.3)-(1.5) were integrated numerically in a doubly-periodic domain. Using $gH_{max} = 9.8\,m^2sec^{-2}$ and taking f at 30^o N (so the inertial period is one day), the Rossby radius a based on H_{max} is about 43Km. For convenience a is used as a length scale, and we define new co-

ordinates

$$(X,Y) = (x,y)/a$$

The topography has

$$H = \begin{cases} \frac{1}{2}H_{max} & 0 < Y < 20 \ , \ 60 < Y < 80 \\ H_{max} & 20 < Y < 60 \end{cases} \qquad (2.22)$$

with period 80 in the Y direction (see Fig. 3). A surface displacement is generated by forcing the height field: the effect is similar to using an initial configuration

$$\eta = \begin{cases} -\eta_o & 0 < X < 20 \ , \ 60 < X < 80 \\ \eta_o & 20 < X < 60 \end{cases} \qquad (2.23)$$

but substantial gravity and inertial wave 'noise' is avoided. Fig. 4a shows contours of η when the forcing is switched off, after two inertial periods. Geostrophic adjustment has led to a jet in the +Y direction along X = 30, and another in the -Y direction along X = 10. The cross-section along Y = 40 shows η effectively unaffected by the steps. Details of part of the velocity field appear in Fig. 4b. Double Kelvin waves can be seen starting to propagate along the steps, in the +X direction at Y = 20, and the -X direction at Y = 60. Note that the wave direction depends on the nature of the step and propagates with the shallow water on the right, and not on the direction of the jet.

After 10 inertial periods the waves have travelled about a quarter of the way across the region, as can be seen in Fig. 5. Flow far from the steps is virtually unchanged, but currents are

diverted along the steps themselves, with very little transport across the steps, consistent with the linearised analysis given above.

3. Numerical results with coast

The preceding results are considerably altered when vertical walls running perpendicular to the steps are added. In this section, time-dependent numerical experiments in a periodic channel are described. The topography is almost identical to (2.22), except that the deep ($H = H_{max}$) region is enlarged to $10 < Y < 60$ to defer interaction of one step with another via coastal Kelvin waves, which travel faster in deeper water. Vertical walls are placed at X=0 and X=-5. Grid spacing is ½a alongshore and a/4 offshore. The height field along X=0 is forced for one 'day' to generate a perturbation: in the absence of the steps this would simply lead to a longshore current near that coast.

The situation after two inertial periods is shown in Fig. 6. Contours of η reveal double Kelvin waves beginning to travel along the steps. (A small amount of gravity wave 'noise' is also apparent, particularly near X=-5, as a consequence of the rather rapid generation.) The cross-section along Y=40, shown to the left of the contour map, effectively shows η as unaffected by the steps. The velocity fields in Figs. 6b,c show the longshore current being deviated toward the coast near (X,Y)=(0,10) and away from the coast near (0,60).

After six inertial periods the double Kelvin waves are well established. The wave travelling away from X=0 along the step at Y=60 has reached the opposite wall: behind it the longshore current has been diverted offshore, with very little flow across the step. Velocity details can be seen in Fig. 7c. The pattern here is similar to that seen in the absence of a wall, in the previous section.

The wave travelling toward X=0 along the step at Y=10 is blocked by the coast. The longshore current there is being pinched into a strong, narrow jet next to the coast, as is evident in the velocity field in Fig. 7b. Strong cyclonic vorticity is generated as the current crosses the step into deeper water; sufficient to create a return flow just offshore. Details here are limited by the resolution of the finite-difference grid, but the flow is confined to the immediate vicinity of the coast. There is very little disturbance further offshore, in contrast to the behaviour at Y=60, where the flow is diverted away from the coast.

After ten inertial periods coastal waves have travelled from one step to the next, and the flows near each step subsequently influence each other. The double Kelvin wave impinging on the wall at X=-5 has generated another coastal wave along that wall, travelling in the -Y direction, as is clear in the contour map in Fig. 8a. The velocity structure near X=0, Y=10, shown in Fig. 8b, seems to be spreading offshore with a complicated pattern of flow reversals; by far the strongest current is still next to the wall however.

4. Steady analytic results with wall

In this section analytic solutions of the linear shallow-water equations are described, for steps supporting double Kelvin waves travelling both toward and away from a vertical coast at x = 0 bounding the semi-infinite region $x \leq 0$.

For steady flow, (1.3) to (1.5) reduce to

$$f v = g \eta_x \tag{4.1a}$$

$$f u = -g \eta_y \tag{4.1b}$$

$$(Hu)_x + (Hv)_y = 0, \tag{4.2}$$

and from (2.4)

$$\frac{\eta}{H} - \frac{\zeta}{f} = \text{initial value} \tag{4.3}$$

For simplicity, we consider an initial surface displacement which is constant to a distance d offshore, and zero thereafter:

$$\eta = \begin{cases} \eta_o & -d < x < 0 \\ 0 & x < -d \end{cases} \tag{4.4}$$

As in section 1, a step runs along y=0, with $H = H_-$ for $y<0$ and $H = H_+$ for $y>0$.

From (4.1)-(4.4),

$$a_\pm^2 \nabla^2 \eta - \eta = \begin{cases} -\eta_o & -d < x < 0 \\ 0 & x < -d \end{cases} \tag{4.5}$$

We choose a_- as a length scale, and define $(X,Y)=(x,y)/a_-$ and $D=d/a_-$.

4.1 No step

For later reference, we first consider the case $H_-=H_+$, for which there is no longshore dependence. Mass conservation requires

$$\int_{-\infty}^{0} \eta \, dX = \eta_o D \tag{4.6}$$

Using this condition, with continuity of η and η_X at $X=-D$ and $\eta \to 0$ as $X \to -\infty$, we obtain

$$\bar{\eta}(X) = \eta_o \sinh D \, e^X + \begin{cases} \eta_o [1-\cosh(X+D)] & -D < X < 0 \\ 0 & X < -D \end{cases} \tag{4.7}$$

(An overbar distinguishes the no-step solution.)

At the coast,

$$\bar{\eta}(0) = \eta_o (1-e^{-D}) = \eta_c \text{ (say)} \tag{4.8}$$

Further, $\bar{\eta}_X = 0$ at $X=0$, so

$$\bar{v}(0) = 0 \tag{4.9}$$

at the coast.

4.2 Double Kelvin wave propagating offshore: $H_- > H_+$

With $H_- > H_+$, double Kelvin waves propagate offshore. Boundary conditions are needed to solve (4.5): in order to obtain

these we first consider the situation as $Y \to -\infty$. Because coastal Kelvin waves transmit information in the +Y direction only (keeping the coast on their right for f>0), we expect $\eta \to \bar{\eta}$ as $Y \to -\infty$. Then, because u = 0 at the coast so η is constant along the wall, it follows that

$$\eta(0,Y) = \eta_c \qquad Y < 0 \tag{4.10a}$$

From (4.1) and (4.2) and continuity of η, it can be deduced that both v and Hv are continuous across the step, which can only be true if v=0 at the step. Thus in the steady state there is no flow across the step, as suggested by the time-dependent numerical experiments. Hence η is constant along the step, and we have

$$\eta(X,0) = \eta_c \qquad X \leq 0 \tag{4.10b}$$

(The double Kelvin wave carries the information $\eta = \eta_c$ away from the coast to set up this state.) Similarly, we find

$$\eta(0,Y) = \eta_c \qquad Y \geq 0 \tag{4.10c}$$

To solve (4.5) in the region Y<0, we put

$$\eta = \bar{\eta} + \phi \tag{4.11}$$

Then

$$\phi_{XX} + \phi_{YY} - \phi = 0 \tag{4.12}$$

with

$$\phi(0,Y) = 0 \qquad Y < 0 \tag{4.13a}$$

$$\phi(X,0) = \eta_c - \bar{\eta}(Y) \qquad X < 0 \tag{4.13b}$$

A solution can be readily obtained using Fourier transforms. In convolution form,

$$\phi = \frac{|Y|}{\pi} \int_{-\infty}^{\infty} F(X-\xi)\, G(\xi,Y)\, d\xi \tag{4.14}$$

where

$$F(X-\xi) = \begin{cases} \eta_c - \bar{\eta}(X-\xi) & \xi > X \\ -\eta_c + \bar{\eta}(\xi-X) & \xi < X \end{cases} \tag{4.15a}$$

and

$$G(\xi,Y) = K_1[(Y^2+\xi^2)^{1/2}]/(Y^2+\xi^2)^{1/2} \tag{4.15b}$$

where K_1 is a modified Bessel function.

Typical shapes of F and G are shown in Fig. 9 to illustrate the nature of the convolution. This form is convenient because G decreases very rapidly as $|\xi|$ increases, so (4.14) can be rapidly evaluated numerically. (It is sufficient to take $|\xi| < 10$ in the following examples.)

Far offshore, as $X \to -\infty$,

$$\eta \to \frac{|Y|}{\pi} \eta_c \int_{-\infty}^{\infty} G(\xi,Y)\, d\xi \tag{4.16}$$

$$= \eta_c e^{Y} \qquad (Y < 0)$$

in agreement with the double Kelvin wave structure discussed in section 2.

We also find that there is a weak flow reversal at the coast. Because $\eta_c - \bar{\eta} > 0$, it follows that $\phi > 0$, with $\phi = 0$ only at the coast. Hence $\phi_X < 0$ at the coast: combining with (4.10), the net effect is $v<0$ at $X=0$, for $Y<0$. (This reversed flow decays to zero as $Y \to -\infty$.)

In the region $Y>0$, a particular solution satisfying (4.5) and (4.10c) is

$$\hat{\eta}(X) = \eta_o [\cosh(\lambda D) - e^{-D}] e^{\lambda X} + \begin{cases} \eta_o [1 - \cosh(\lambda(X+D))] & -D < X < 0 \\ 0 & X < -D \end{cases} \qquad (4.17)$$

where

$$\lambda = a_-/a_+ = (H_-/H_+)^{1/2} \quad .$$

The complete solution for η can then be obtained in convolution form as for the region $Y<0$, with $\eta \to \hat{\eta}$ as $Y \to -\infty$. Note that $\hat{\eta}_X < 0$ at $X=0$, so there is a flow reversal at the coast associated with the particular solution. This far-field flow reversal is caused by Kelvin waves carrying information from the step along the wall in the +Y direction.

The surface displacement η is shown in Fig. 10, for $H_-/H_+ = 2$, and initial perturbation width $D=1$. The contours of η are streamlines, and arrows indicate the direction of flow when $\eta_o > 0$. (The arrows are reversed if $\eta_o < 0$.) Weak flow reversal

near the coast is evident in the enlargement of the step/coast intersection in Fig. 10b. In this case the step could be replaced by a wall, and the region $Y<0$ would be unchanged. Thus this solution is analogous to deflection of a Kelvin wave around a corner (cf Buchwald 1968).

4.3 Double Kelvin wave propagating onshore: $H_- < H_+$

Again $\eta \to \bar{\eta}$ as $Y \to -\infty$, so the boundary condition (4.10a) still holds. Along $Y=0$, η is constant as before, with no large-scale flow over the step. In this case, however, the constant is determined by double Kelvin waves carrying the information $\eta = 0$ toward the coast from far offshore, and in the steady state

$$\eta(X,0) = 0 \qquad X < 0 \ . \tag{4.18}$$

(This condition is consistent with the numerical results, and with time-dependent calculations which are the subject of a separate paper in preparation.) There is a singularity where the step meets the coast: it arises as a thinning boundary layer in the time-dependent case. In practise, inertial and viscous (and finite-difference) effects set up a narrow boundary layer.

The constant value of η at the coast for $Y>0$ can be found from mass conservation as follows. The transport across a line between two points A and B (say) in a region of depth H is

$$\frac{gH}{f}(\eta_A - \eta_B) \tag{4.19}$$

Thus there is a transport $gH_-\eta_c/f$ from the region $Y<0$ across the step via the singular region. This transport is balanced in the region $Y>0$ if

$$\eta(0,Y) = \frac{H_-}{H_+}\eta_c \qquad Y > 0 \ . \tag{4.20}$$

For the region $Y<0$ we put $\eta = \bar{\eta} + \phi$ as before, and solve (4.12) with

$$\phi(0,Y) = 0$$

$$\phi(X,0) = -\bar{\eta}$$

to obtain

$$\phi = \frac{|Y|}{\pi}\int_{-\infty}^{\infty} F(X-\xi)\,G(\xi,Y)\,d\xi \; - \; \frac{2|Y|}{\pi}\eta_c \int_X^0 G(\xi,Y)\,d\xi \tag{4.21}$$

The first integral is the well-behaved solution obtained previously; the singular behaviour is contained in the second integral. The nature of this term is more apparent for $X^2 + Y^2 \ll 1$, when

$$\frac{-2|Y|}{\pi}\eta_c \int_X^0 G(\xi,Y)\,d\xi \approx \frac{2}{\pi}\eta_c \arctan(X/|Y|) \tag{4.22}$$

This expression approaches 0 as $X/|Y| \to 0$, and approaches $-\eta_c$ as $|Y|/X \to 0$.

For the region $Y>0$ we assume that (4.5) still applies. In practice, this equation may not apply everywhere due to the possibly substantial advection of potential vorticity across the step, further modified by boundary layer effects. Our solution using (4.5) should be regarded as a first approximation for a more complicated situation.

The particular solution satisfying (4.5) and (4.20) is

$$\tilde{\eta}(X) = \eta_o [\cosh(\lambda D) - 1 + \lambda^2 (1 - e^{-D})] e^{\lambda X} + \qquad (4.23)$$

$$+ \begin{cases} \eta_o [1 - \cosh(\lambda(X+D))] & -D < X < 0 \\ 0 & X < -D \end{cases}$$

A solution in convolution form can then be found as before.

Fig. 11 shows η for the case $H_-/H_+ = 0.5$, and $D = 1$. The effect of the step is now chiefly confined to the coastal region, in contrast to the outgoing wave case. For $Y<0$, there is no flow reversal, and all streamlines pass through (0,0). In this case flow reversal does appear in part of the region $Y>0$.

5. Laboratory experiments

In this section we report on some laboratory experiments which illustrate the phenomena described in the earlier parts of this paper. These experiments were carried out in a rectangular channel 1.53 m long, 29.4 cm wide and 15.2 cm deep, which was mounted on a direct-drive rotating turntable. The channel was centered on the vertical axis of rotation of the turntable. Inserts constructed from polystyrene blocks were placed on the bottom of the channel to produce a variety of different types of bottom topography. In the experiments described here a rectangular block covering one-half the base of the tank and 5 cm in height was used to produce the step change in depth considered in the theoretical calculations.

Geostrophic adjustment of a two-layer fluid was examined, with the initial discontinuity in the interface height produced by a thin vertical barrier running the length of the tank a distance L from one of the side walls. Salt solution of the required density was first placed in the channel and the system spun up to solid body rotation. A layer of fresh water was then carefully floated on top. The barrier was then placed in position and a further amount of fresh water containing some dye for flow visualisation was added in the thin region between the barrier and the tank wall. The whole system was then left to come to solid-body rotation with angular velocity $\Omega = \frac{1}{2}f$, a process which took about an hour. This initial configuration is shown on Fig. 12. The experiment was initiated by the vertical removal of the barrier.

The flow was observed by the movement of the dye in the upper layer and from the motion of small paper particles

scattered on the free surface. In a few experiments patches of dye were also added to the lower layer in an attempt to infer the flow in that layer. Photographs of the flow were taken during the course of the experiment with a camera mounted in the rotating frame.

The depth of the lower layer was in the range 9-14 cm at the deep end and 5-9 cm at the shallow end. The upper layer depth was 1-3 cm and the difference in the upper layer depth on the two sides of the barrier, corresponding to η_o of (1.1), varied between 2-4 cm. The values of the reduced gravity $g' = g\Delta\rho/\rho$ between the two layers was varied from 1-21 cm s^{-2} and the Coriolis parameter f took values from 0.5-3 s^{-1}. The initial width L of the region between the barrier and the wall varied from 2.5-10 cm. The dimensionless initial width L/a, where a is the Rossby radius, took values in the range 0.7-3.1

A number of experiments were also carried out with a two-layer stratification on the shoreward side of the barrier only (i.e. h =0 on Fig. 12). In this case the geostrophic adjustment in the absence of topography produces a coastal current, the outer edge of which is bounded by a density front at a position approximately L + a from the wall (Griffiths & Linden 1982). As in the two-layer case adjustment produces a flow parallel to the wall with the upper-layer flow directed so that the wall is on the right when facing downstream for f>0. A flow is also induced in the lower layer but in the opposite sense.

Both the two-layer and frontal currents are unstable to wave-like perturbations which grow along the length of the current. These instabilities grow to large amplitude and form regions of closed streamlines in about 10 rotation periods and appear to

gain much of their energy from the sloping density interface remaining after adjustment (Griffiths & Linden 1982, Killworth, Stern & Paldor, 1984). The initial adjustment and formation of the coastal current occurs within 1 or 2 rotation periods. For the present purposes the presence of the instabilities produces undesirable noise, as we are interested in the mean flow and transport in the current and the response of this to the change in the fluid depth. Unfortunately, the instabilities are unavoidable in the parameter ranges required to demonstrate the phenomena and they obscure some of the more subtle features of the flow predicted by the analysis.

5.1 Two-layer flows

A sequence of photographs showing the motion of the upper layer in a two-layer flow is shown on Fig. 13. In this example the upper-layer flow induced by the adjustment is towards the shallow end of the tank, which is on the right of the picture. The double Kelvin wave, which propagates with the deeper water on the left, travels across the tank above the step in the direction away from the coast. Thus the current in the upper layer approaching the step from the left is diverted away from the wall and into the interior of the tank. On reaching the far wall (Fig. 13c) the flow is diverted along that wall by a coastal Kelvin wave. The speed of advance of the dyed fluid is approximately 1 cm s^{-1}, which is consistent with that of the Kelvin wave given by (2.18). The flow in the lower layer, although not shown in this example, is in the opposite direction. This flow approaches the step from the left (the shallow end) and is diverted out into the interior of the tank by the double Kelvin wave. The width of the diverted flow is observed to be

approximately 15 cm, which is about twice the Rossby radius (7.4 cm). This result is consistent with the analytical and numerical calculations, and was found to hold for all the other values of the parameters studied.

It is not possible to say whether the step acts as a total barrier to the flow as is suggested by the theoretical calculations. There appears to be little flow across the step as can be seen by the reduction in width in the dyed fluid immediately downstream of the step visible on Fig. 13c, but the presence of the instabilities makes it impossible to determine the exact nature of the flow in the vicinity of the step and the wall.

The case where the flow upper layer is approaching the deep end of the tank is shown on Fig.14. The upper layer is again flowing from left to right, and the double Kelvin wave over the step propagates towards the wall. This case is even more contaminated by the instabilities, since the effect of the Kelvin wave is confined to the region near the wall and the current where the growing waves occur. However, evidence can be seen for an indentation in the dye over the step which increases in size (Figs.14b & 14c) until it is swamped by the instabilities in the current. The flow across the step is confined to a thin boundary layer near the wall.

5.2 Frontal flows

Similar features were observed in the flow over a step of a coastal current bounded by a front. The two cases are shown in Fig.15. In Fig. 15a the upper layer is approaching the shallower end and the double Kelvin wave propagates across the tank away from the wall. The opposite case is shown on Fig. 15b where

the upper layer is approaching the deep end (the flow of dyed fluid is from right to left and $f<0$) and the Kelvin wave travels in towards the wall. In this example the reduction in thickness of the current is clearly visible, and the cross-step flow is confined to a thin region near the wall. Again the presence of instabilities makes it impossible to detect features such as the weak recirculating region near the step, predicted by the theoretical calculations (see Fig 10).

The similarities between the frontal flows and the two-layer adjustment suggests that the basic aspects of the flow in the presence of topography are robust. In the frontal case the diversion of the flow into the interior of the fluid by the step can only be achieved by advection of fluid particles, since there is no initial stratification to support an internal double Kelvin wave. The preceding theory, dealing only with small displacement of fluid particles, does not address this case but the similarity between the two types of experiment suggest that it does describe the basic dynamics of these large amplitude motions.

6. Summary

The effects of step-like topography on geostrophic adjustment have been examined using laboratory experiments and theory based on the linear shallow-water equations. We find that flow normal to the step is diverted into flow along the step, forming a double Kelvin wave which propagates only in the direction with deeper water to the left. The speed of this wave is the difference between the gravity wave speeds oneither side of the step. An important result is that transport across the step effectively only occurs at the propagating wave front. Only material located near the step (along the step in the linear limit) can cross; otherwise the step acts as a complete barrier to approaching flow.

The direction of propagation of the double Kelvin wave also determines the effect of a vertical wall representing a coast. If the geometry allows offshore propagation, then the wall has very little additional effect: any longshore flow is simply diverted along the step away from the wall. However, if double Kelvin waves travel onshore, then flow along the step is blocked and a thin boundary layer forms, within which an intense jet can transport fluid across the step into a coastal current.

Laboratory experiments were carried out with a step across a rotating channel containing two layers of fluid of different density. An alongshore current was either diverted offshore along the step or 'pinched' into a boundary layer, with speeds and horizontal scales in broad agreement with theory. Instability of the alongshore current obscured many details however, particularly of the quantitative flow across the step. Strictly, the shallow-water theory only applies with a relatively deep upper

layer, and a two-layer theory is required, but the laboratory results show that the main phenomena can be qualitatively explained by the simple model described here.

In some experiments fronts intersecting the free surface were used. Again, behaviour is qualitatively like the simple model, but in this case material transport is important and a more complete theory must take non-linear advection effects into account. Further laboratory and numerical work with a variety of slopes, rather than steps (not described here), also shows similar features: generally, a broader slope simply gives lower wave speeds and broader disturbances along the slope.

Detailed analysis of the boundary layer 'pinched' next to the wall has not been made. Such work should properly include viscous and advective effects because a material column crossing the step needs to alter its potential vorticity in some way.

Apart from numerical calculations, details of time-dependent flow have not been given. An analytic rigid-lid solution by Johnson (1985) is relevant to a double Kelvin wave impinging on a wall; analytic free-surface calculations with and without a wall have been made and a separate paper is in preparation.

References

Buchwald, V.T. (1968) The diffraction of Kelvin waves at a corner. J. Fluid Mech. 31, 193-205.

Gill, A.E. (1982) Atmosphere-Ocean Dynamics. Academic Press. 666 pp.

Griffiths, R.W. & P.F. Linden (1982) Laboratory experiments on fronts. Part 1. Density-driven boundary currents. Geophys. Astrophys. Fluid Dynamics 19, 159-187.

Hsieh, W.W. & A.E. Gill (1984) The Rossby adjustment problem in a rotating, stratified channel, with and without topography. J. Phys. Oceanogr. 14, 424-437.

Johnson, E.R. (1985) Topographic waves and the evolution of coastal currents. J. Fluid Mech. 160, 499-509.

Longuet-Higgins, M.S. (1968) On the trapping of waves along a discontinuity of depth in a rotating ocean. J. Fluid Mech. 31, 417-434.

Rossby, C.G. (1937) On the mutual adjustment of pressure and velocity distributions in certain simple current systems. I. J. Mar. Res. 1, 15-28.

Rossby, C.G. (1937) On the mutual adjustment of pressure and velocity distributions in certain simple current systems. II. J. Mar. Res. 2, 239-263.

Willmott, A.J. (1984) Forced double Kelvin waves in a stratified ocean. J. Mar. Res. 42, 319-358.

Figure Captions

Fig.1. Geometry and initial surface configuration for adjustment over a step. There is a jump in surface displacement along $x = 0$, and in bottom topography along $y = 0$.

Fig.2. A sketch of contours of surface displacement in the region $y < 0$ after release of the initial configuration in Fig.1. A double Kelvin wave is travelling in the $+x$ direction: details of the flow in the vicinity of dashed contours have not been calculated.

Fig.3. Geometry and effective initial surface configuration for the doubly-periodic numerical experiment. The length unit is the Rossby radius a for the deep region.

Fig.4. The flow corresponding to Fig.3 after two inertial periods.

(a) Surface contours of surface displacement η (negative dashed, zero dotted). Cross sections along the arrowed positions appear to the left and below the contour map.

(b) Details of the horizontal velocity field near the step along $x/a = 20$ where a double Kelvin wave is beginning to propagate in the $+x$ direction.

Fig.5. As for Fig.4, but after ten inertial periods

(a) surface displacement η ; (b) details of velocity field.

Fig.6. The numerical experiment in a periodic channel, after two inertial periods. There are walls at $x/a = 0$ and -5 , and steps at $y/a = 10$ and 60 , with deep water for $10 < y/a < 60$.

(a) surface displacement η ;

(b) velocity field near $y/a = 10$, where a double Kelvin wave propagates toward the wall at $x = 0$;

(c) velocity field near $y/a = 60$, where a double Kelvin wave

propagates away from $x = 0$.

Fig.7. As for Fig.6, but after six inertial periods.

(a) surface displacement;

(b) velocity field near $y/a = 10$, where there is strong longshore flow at the step/wall intersection;

(c) velocity field near $y/a = 60$.

Fig.8. As for Fig.6, but after ten inertial periods.

(a) surface displacement;

(b) velocity field near $y/a = 10$;

(c) velocity field near $y/a = 60$.

Fig.9. The functions F and G as defined in equation (4.15) for the convolution integral, for $X = Y = -2$.

Fig.10 Contours of surface displacement η for the steady state with $H_-/H_+ = 2$.

(a) large-scale view,

(b) enlargement of the step/wall intersection, showing regions of reversed flow;

Arrows on contours indicate flow direction for an initially positive disturbance to η.

Fig.11 Contours of surface displacement η for the steady state with $H_-/H_+ = 0.5$.

Fig.12 A sketch of the experimental set up. The experiment is initiated by removing the vertical barrier.

Fig.13 The adjustment of a two-layer flow when the upper layer is approaching the shallow end. The dyed fluid is in the upper layer and was initially confined to the region between the barrier and the wall. The flow across the tank set up by the double Kelvin wave above the step is clearly visible. The plan-view photographs are taken at 2,3 and 6 rotation periods after the barrier is removed. The flow in the upper layer is from left to right, and the growth of instabilities on the

interface can also be seen. In this experiment L = 8cm, h_1 = 2cm, η_o = 3cm, h_2 = 9cm, g' = 21cm s^{-2} and f = 1.27s^{-1} . The scale on the floor of the tank is in 10cm squares.

Fig.14 The adjustment of a two-layer flow when the upper layer is approaching the deep end. In this case the double Kelvin wave propagates in towards the wall and the thinning of the current in the vicinity of the step can be seen. The photographs are taken at 2, 3 and 4 rotation periods after the removal of the barrier. The parameters are L = 5cm, h_1 = 2cm, η_o = 2cm, h_2 = 9cm, g' = 21cm s^{-1} and f = 1.20 s^{-1}.

Fig.15 The adjustment of a coastal current bounded by a front.

(a) The current of dyed upper-layer fluid is propagating from left to right as it approaches the shallow end and is diverted across the tank over the step. The full width (29.4cm) of the tank is shown. In this experiment L = 5cm, h_1 = 0, η_o = 2.5cm, h_2 = 10.5cm, g' = 10cm s^{-2} and f = 2.5 s^{-1} .

(b) In this case f < 0 and so the coastal current propagates from right to left and the double Kelvin wave travels towards the coast over the step. L = 5cm, h_1 = 0, η_o = 2.5, h_2 = 10.5cm, g' = 10cm s^{-1} and f = -2.5 s^{-1} .

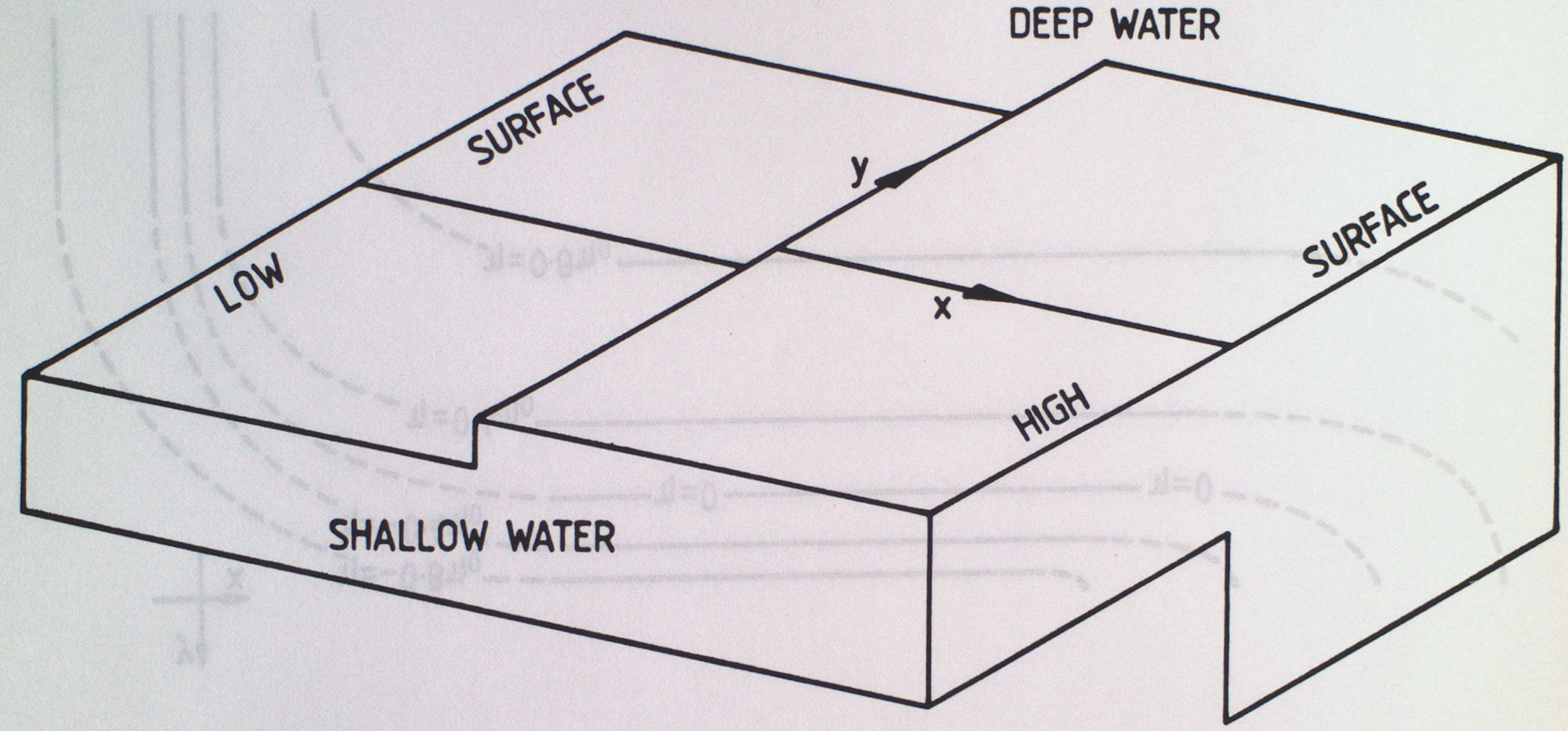

Fig. 1

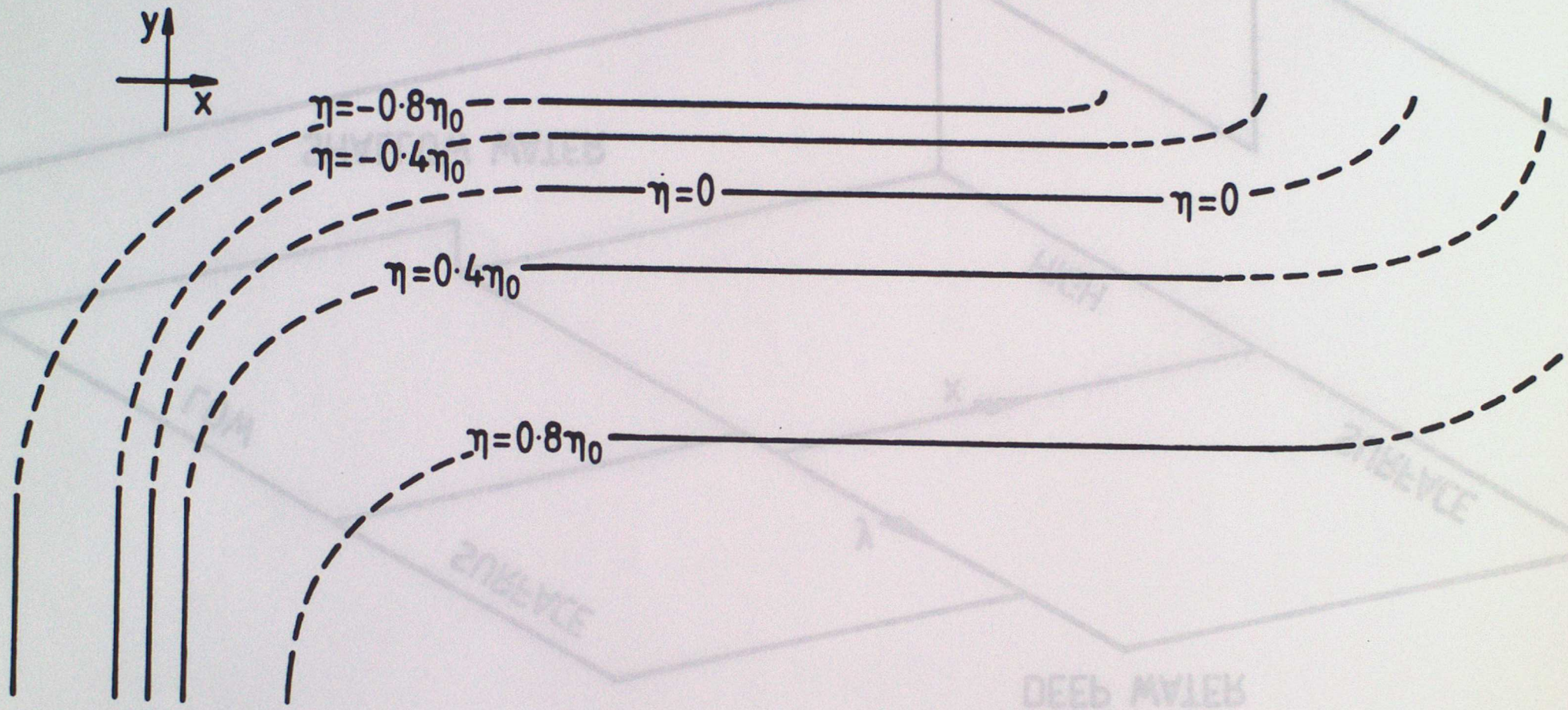

Fig. 2

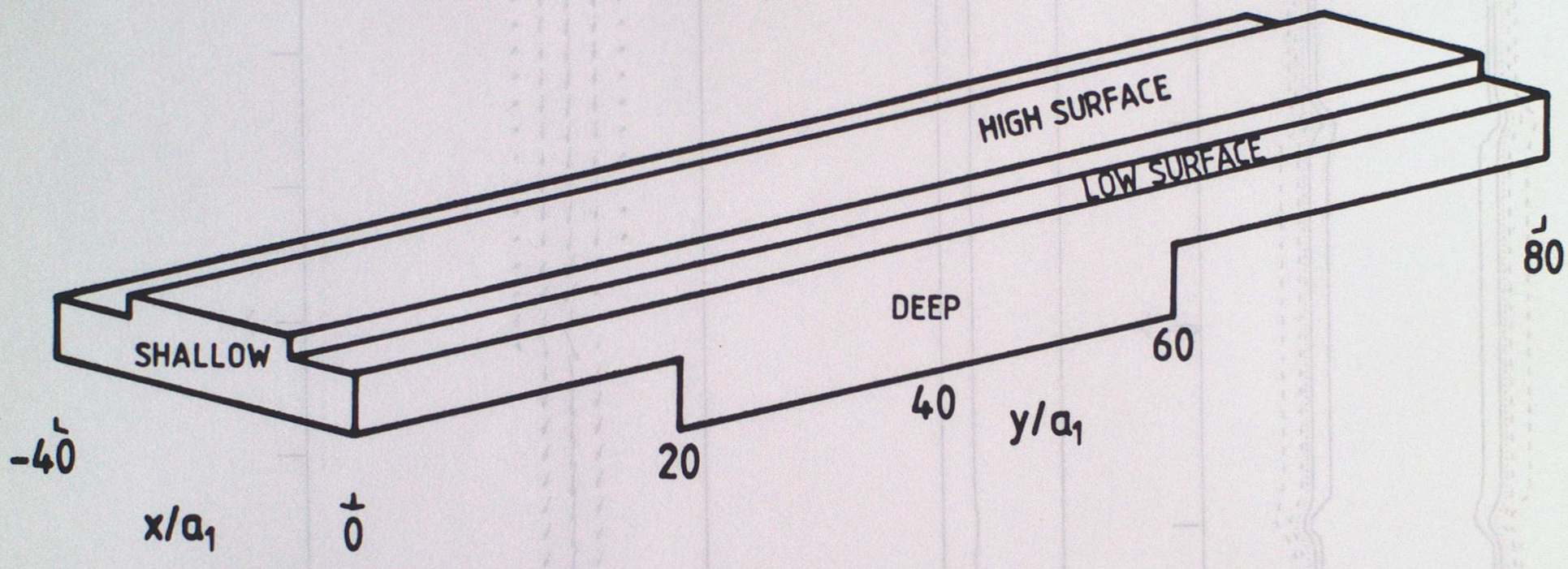
HIGH SURFACE
LOW SURFACE
SHALLOW
DEEP
-40
0
20
40
60
80
x/a1
0
y/a1

Fig. 3

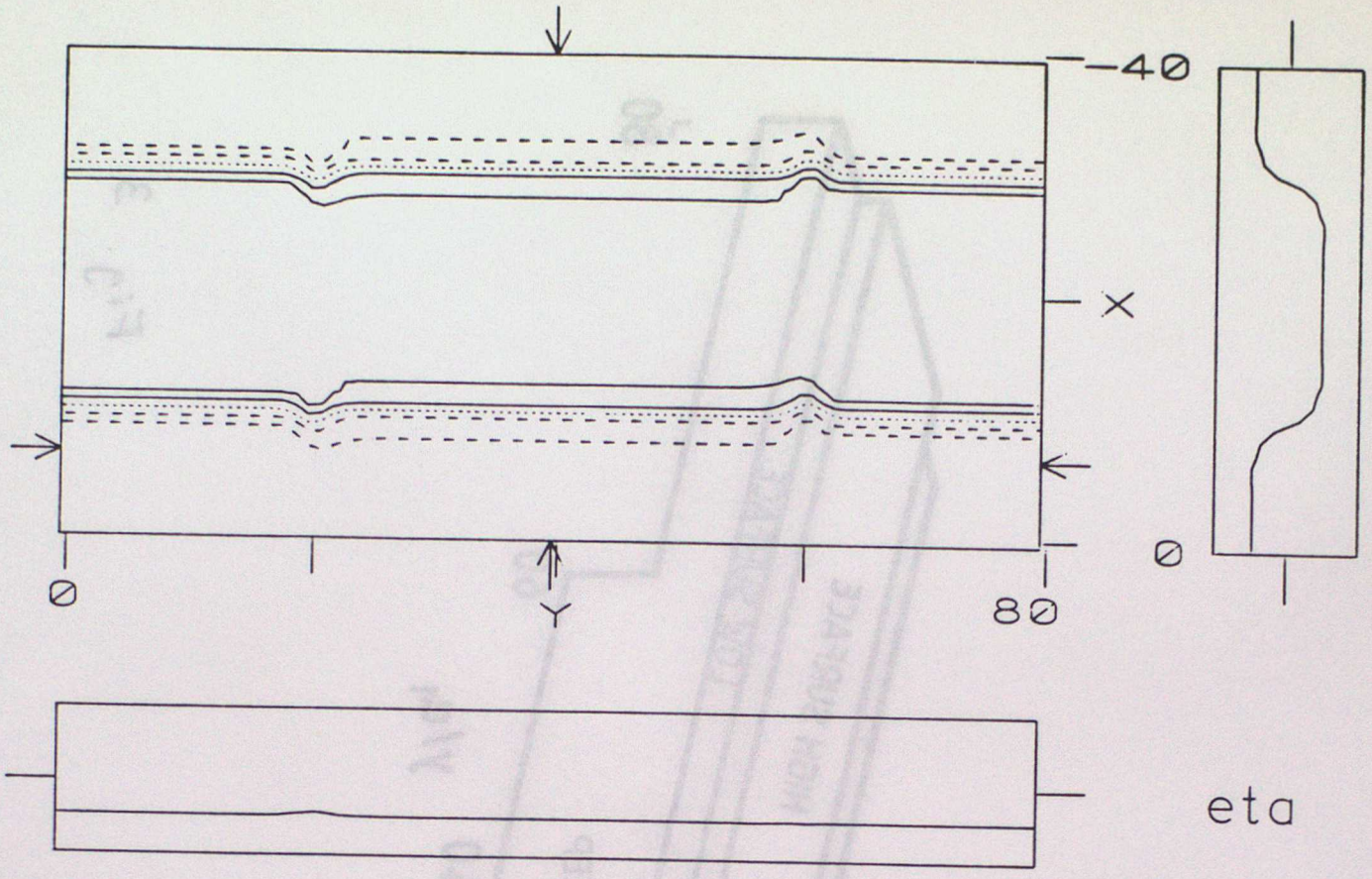

Fig. 4a

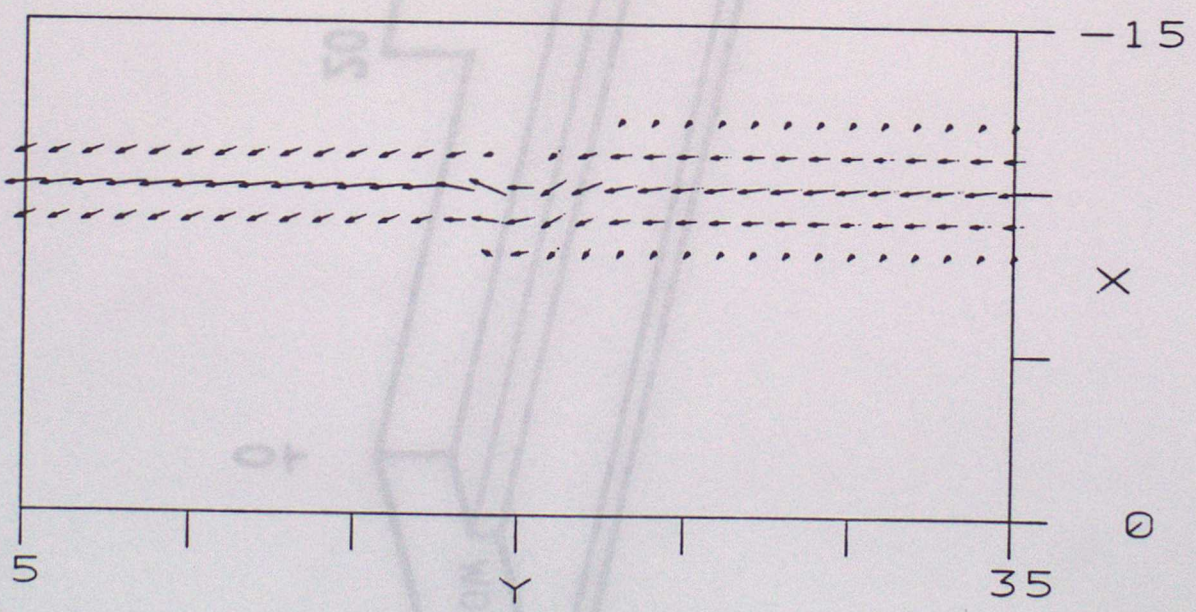

Fig. 4b

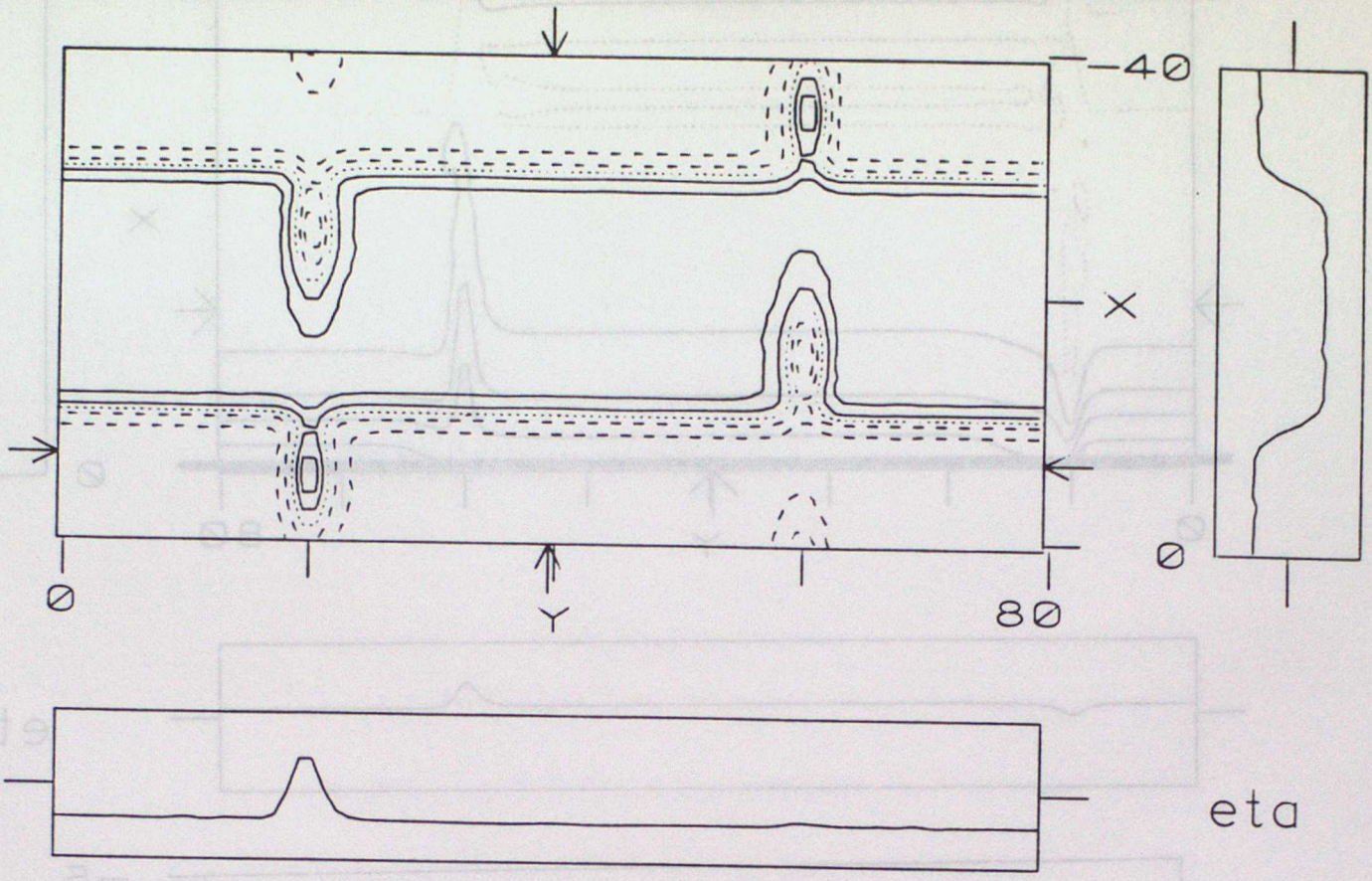

Fig. 5a

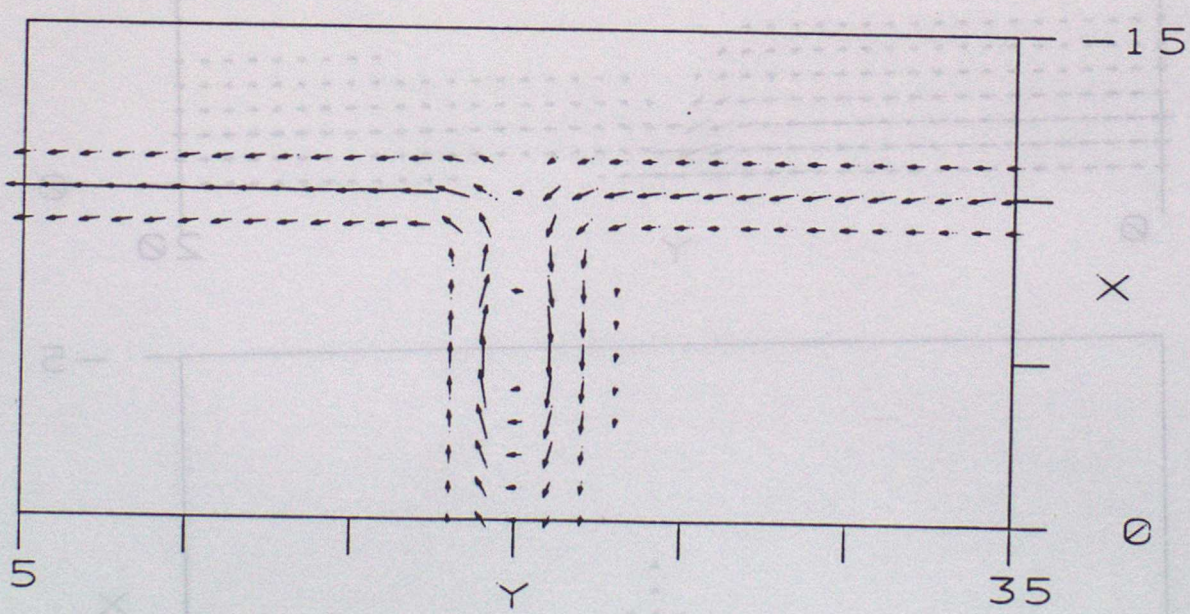

Fig. 5b

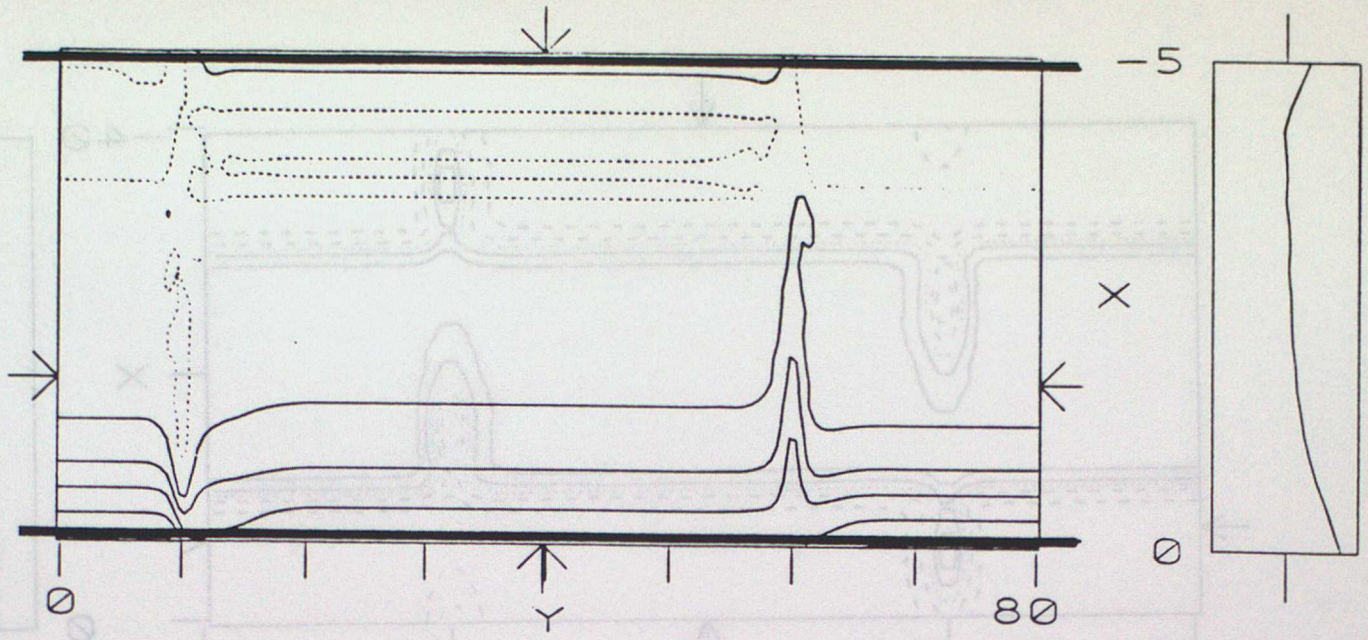

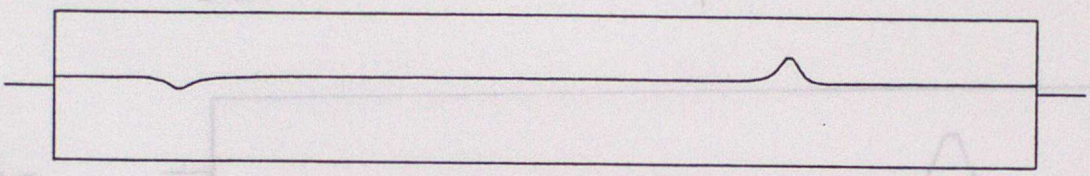

Fig. 6a

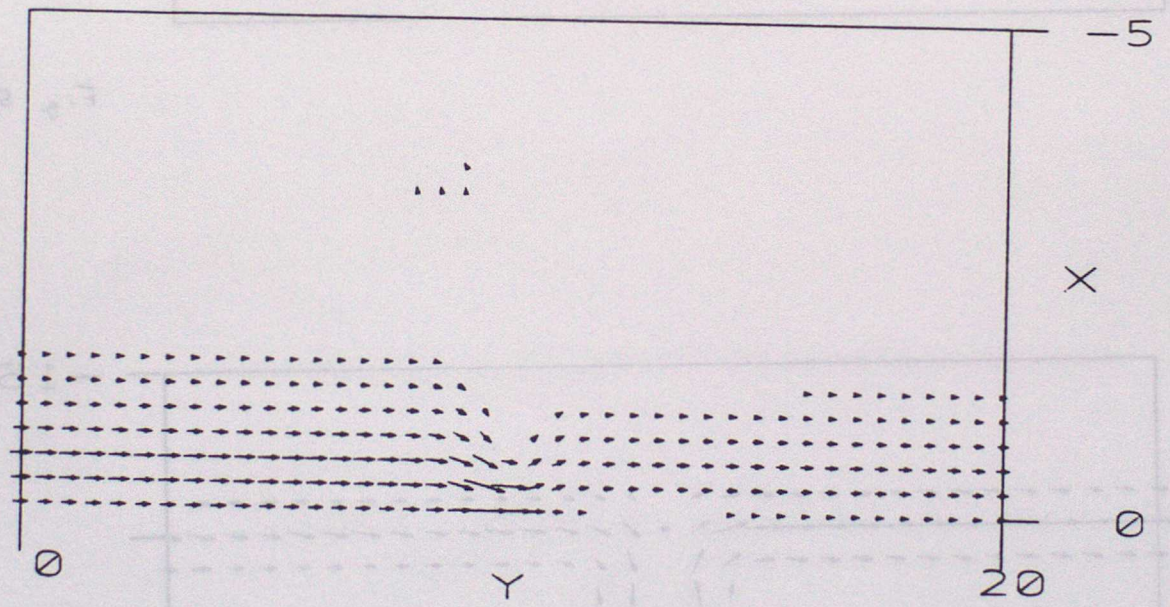

Fig. 6b

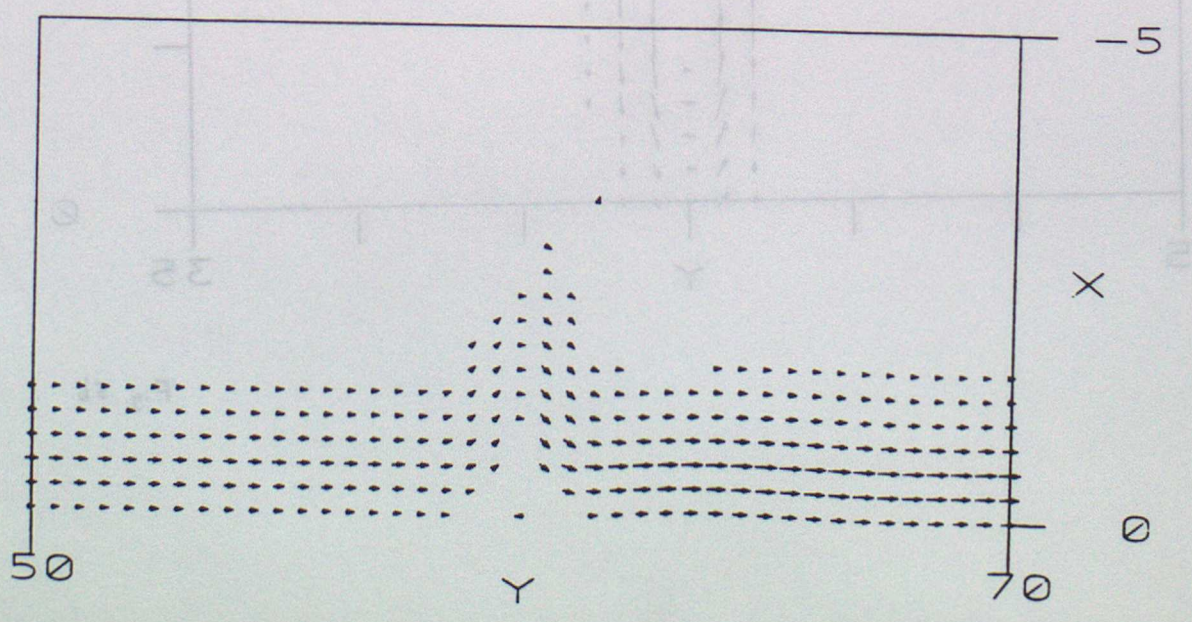

Fig. 6c

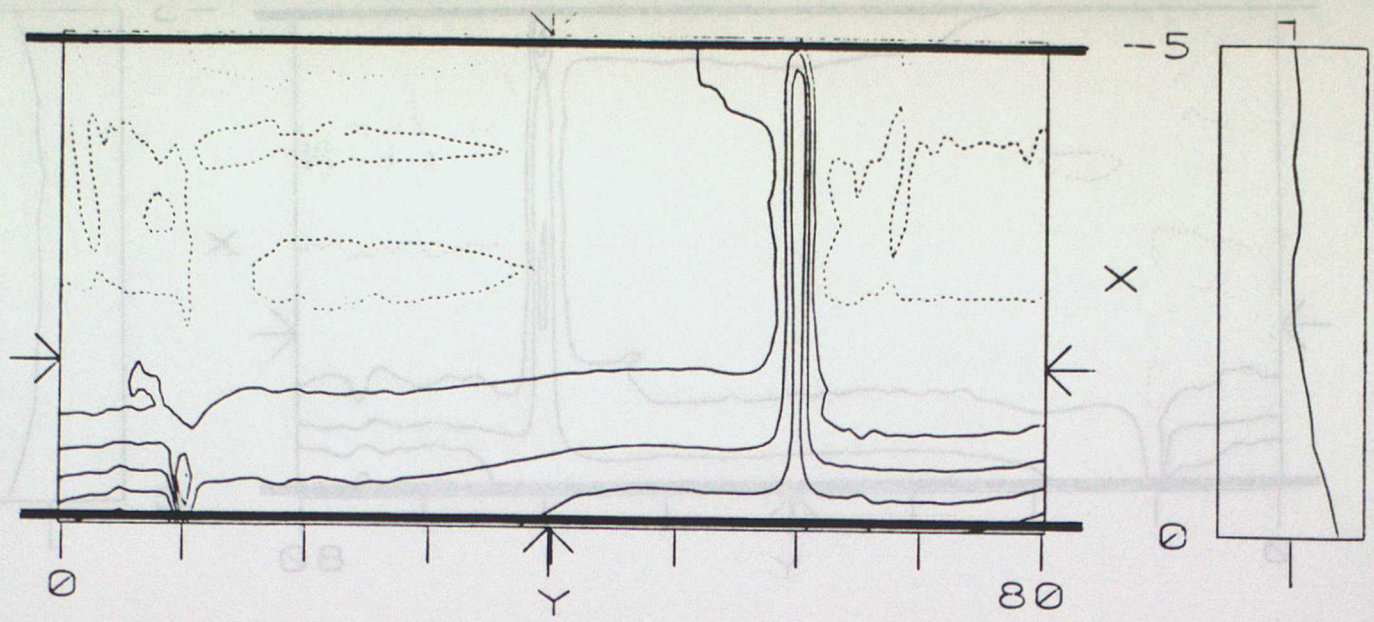

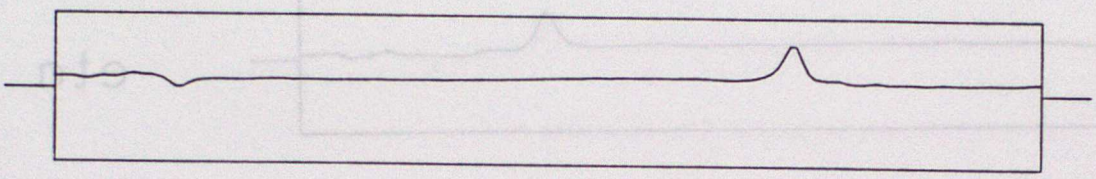

Fig. 7a

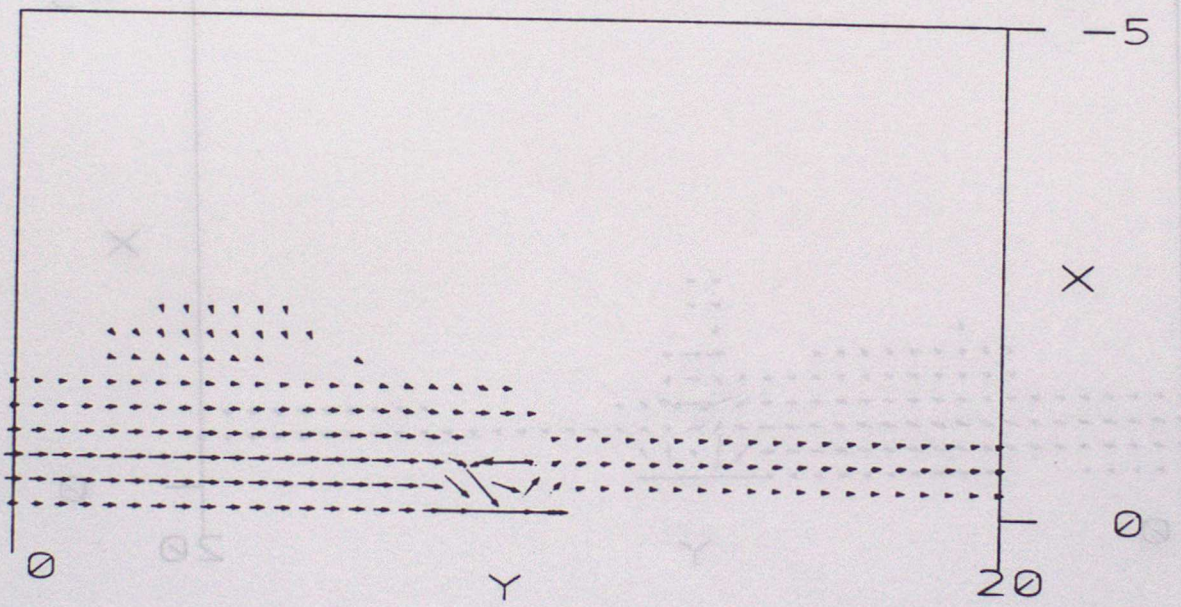

Fig 7b

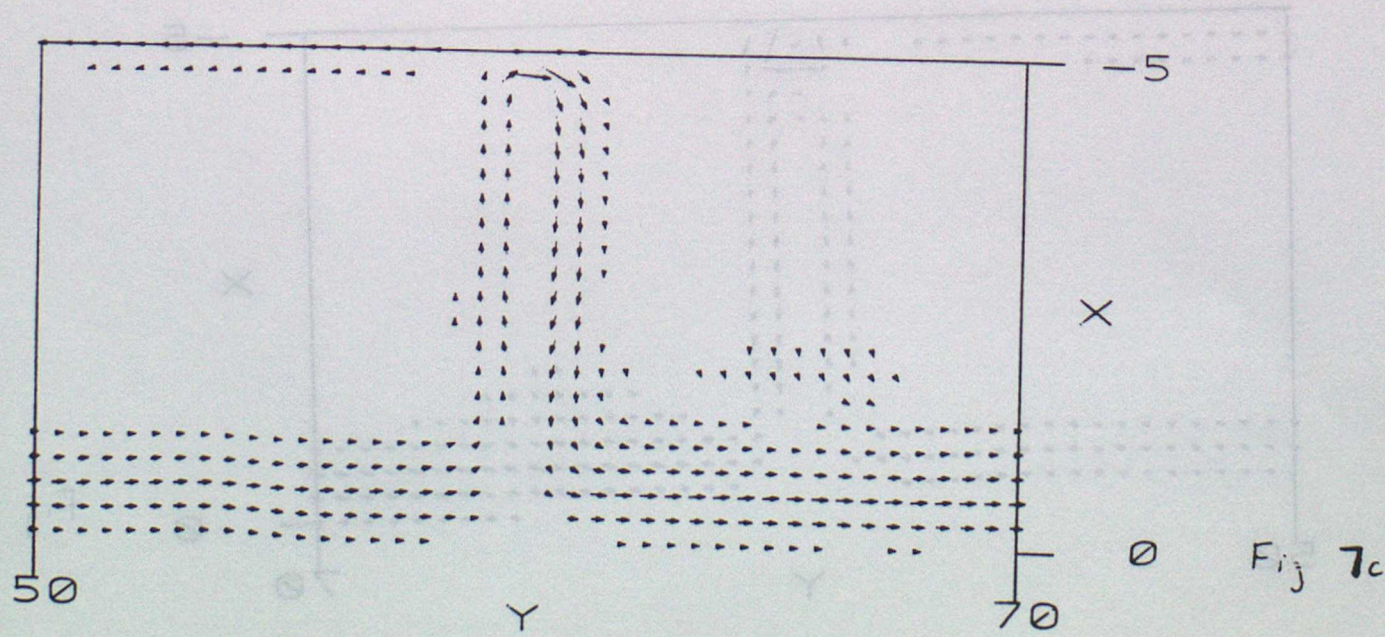

Fig 7c

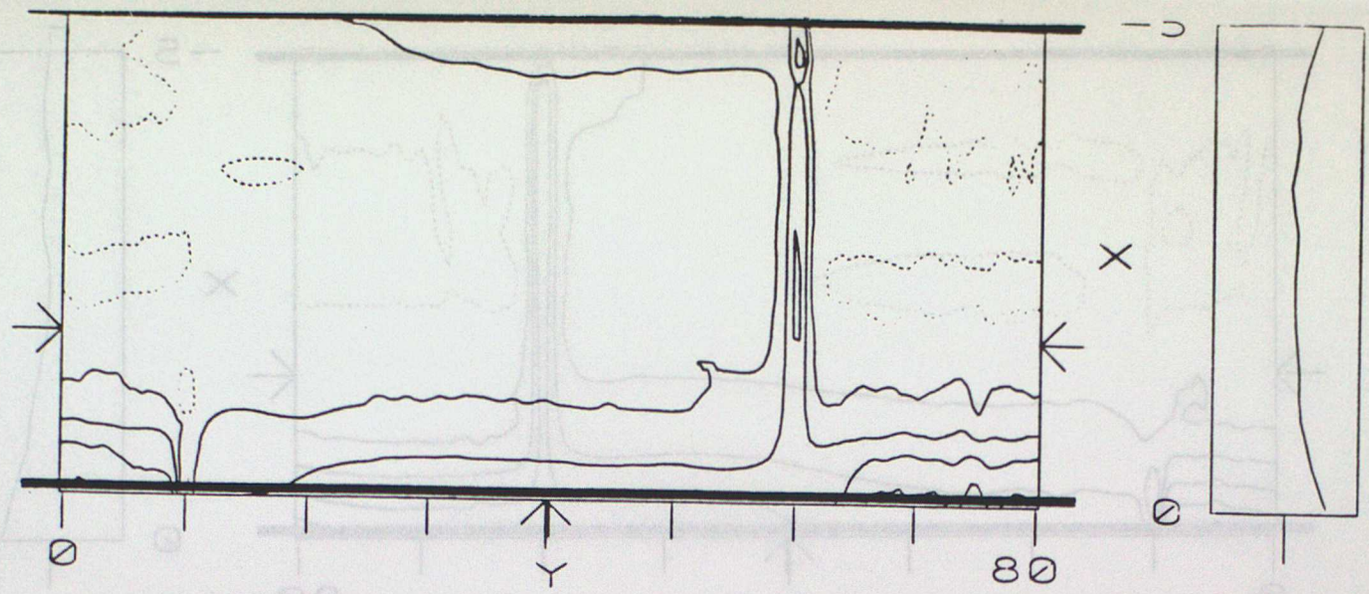

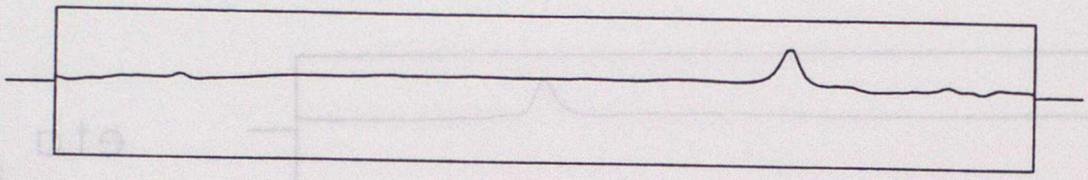

eta

Fig 8a

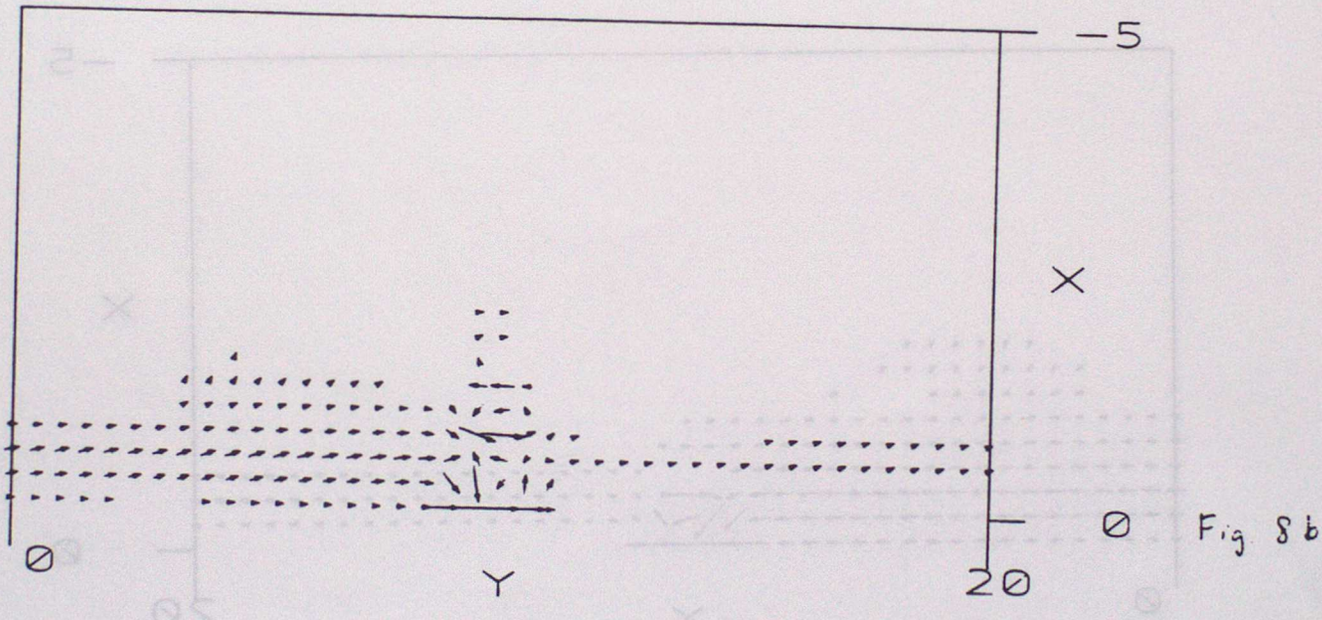

Fig 8b

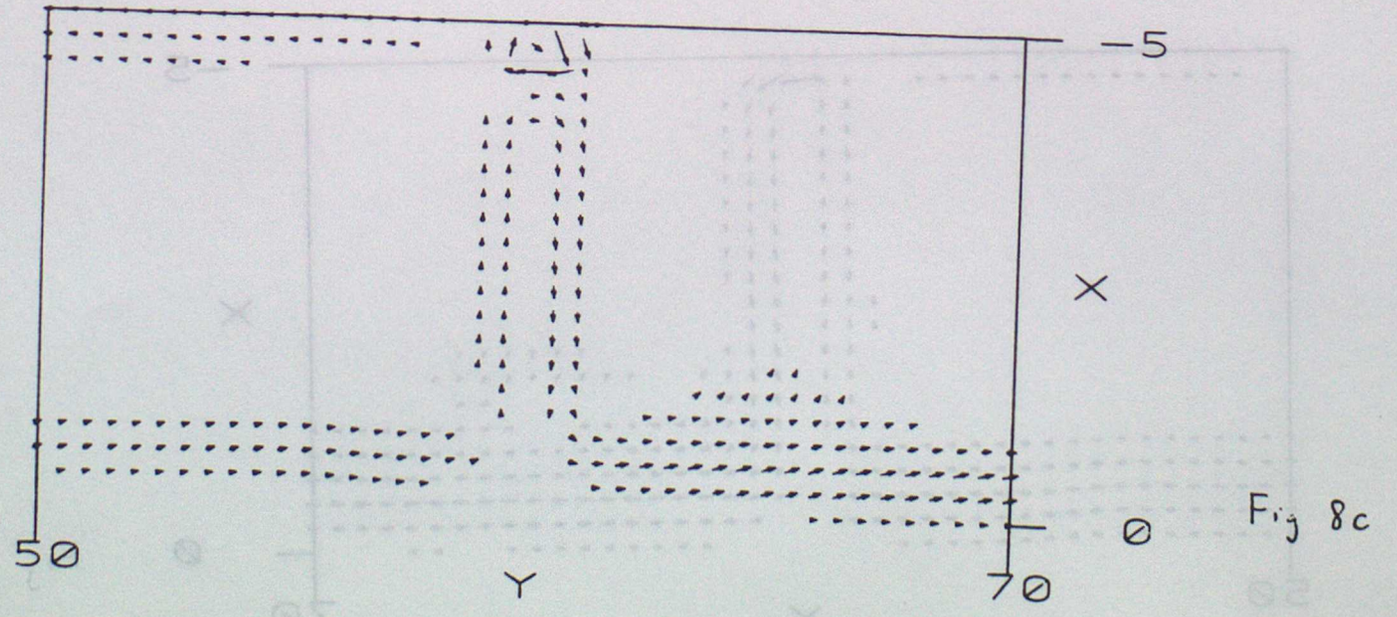

Fig 8c

Fig 8c

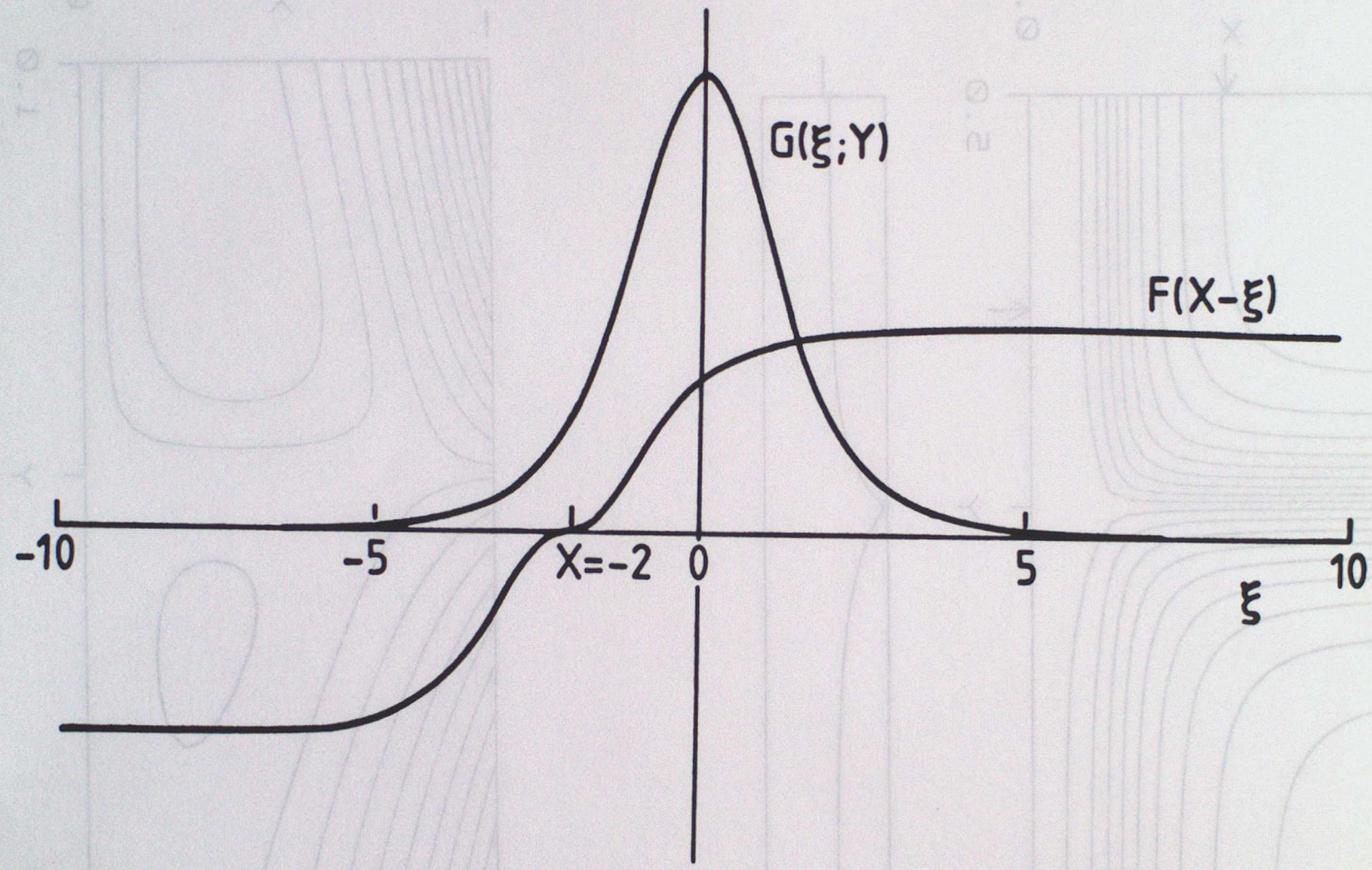

Fig. 9

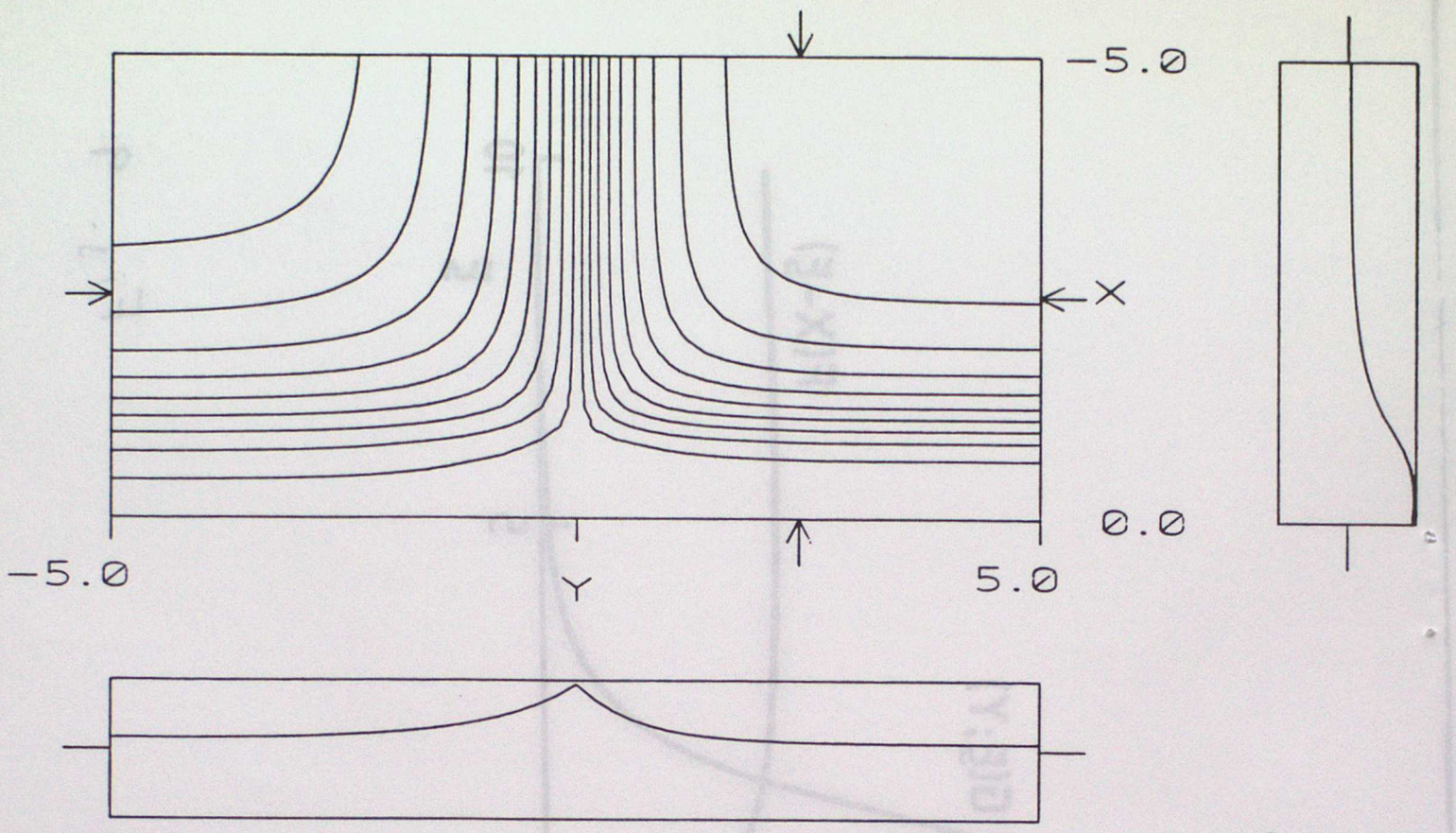

Fig 10a

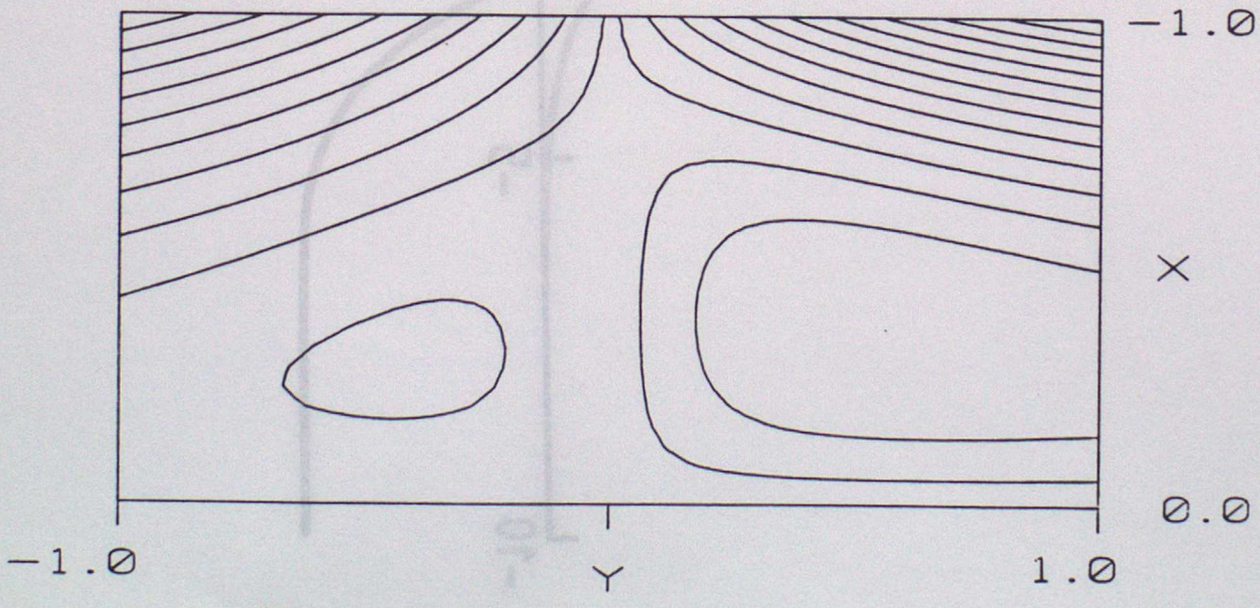

Fig. 10b

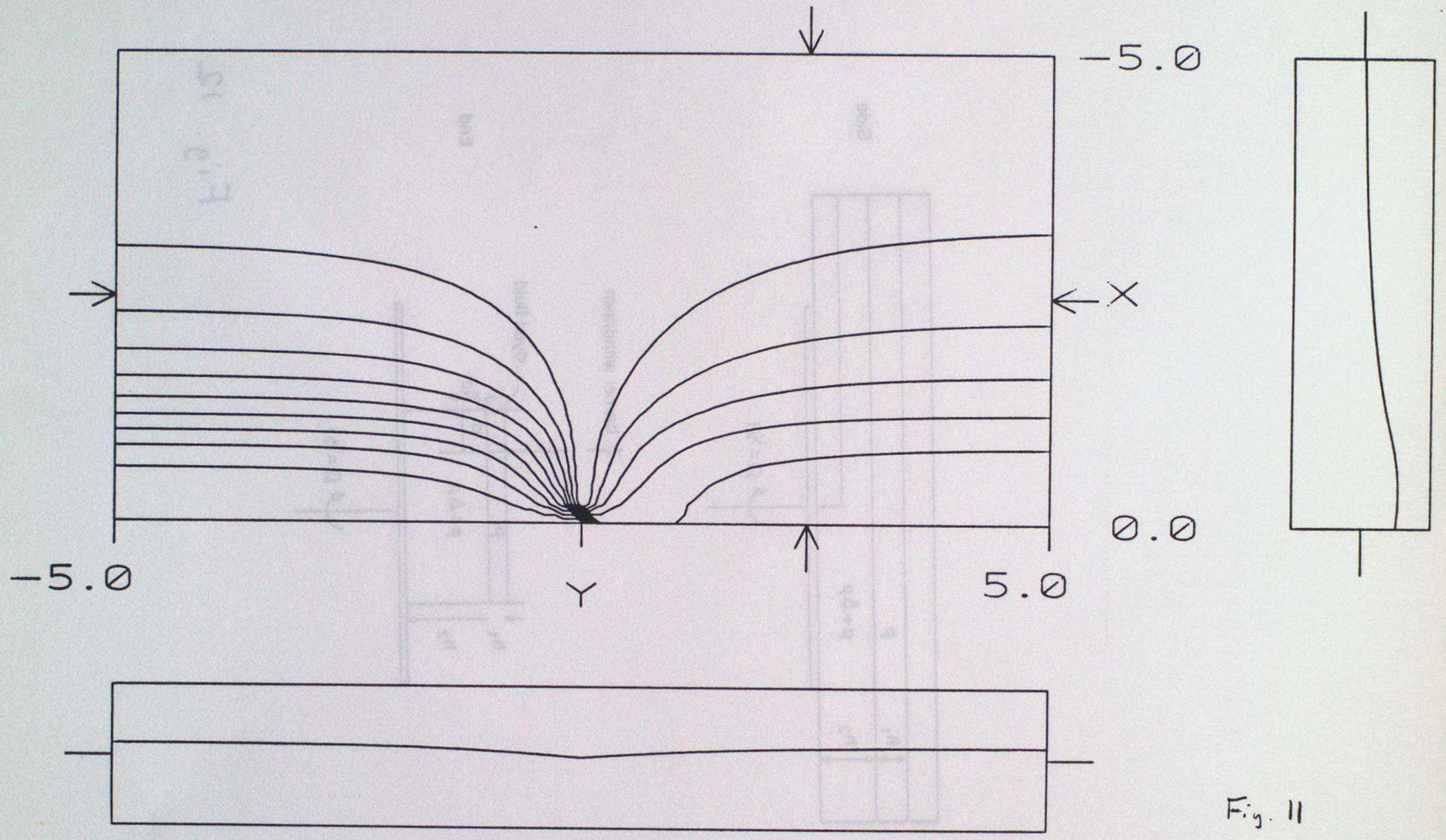

Fig. 11

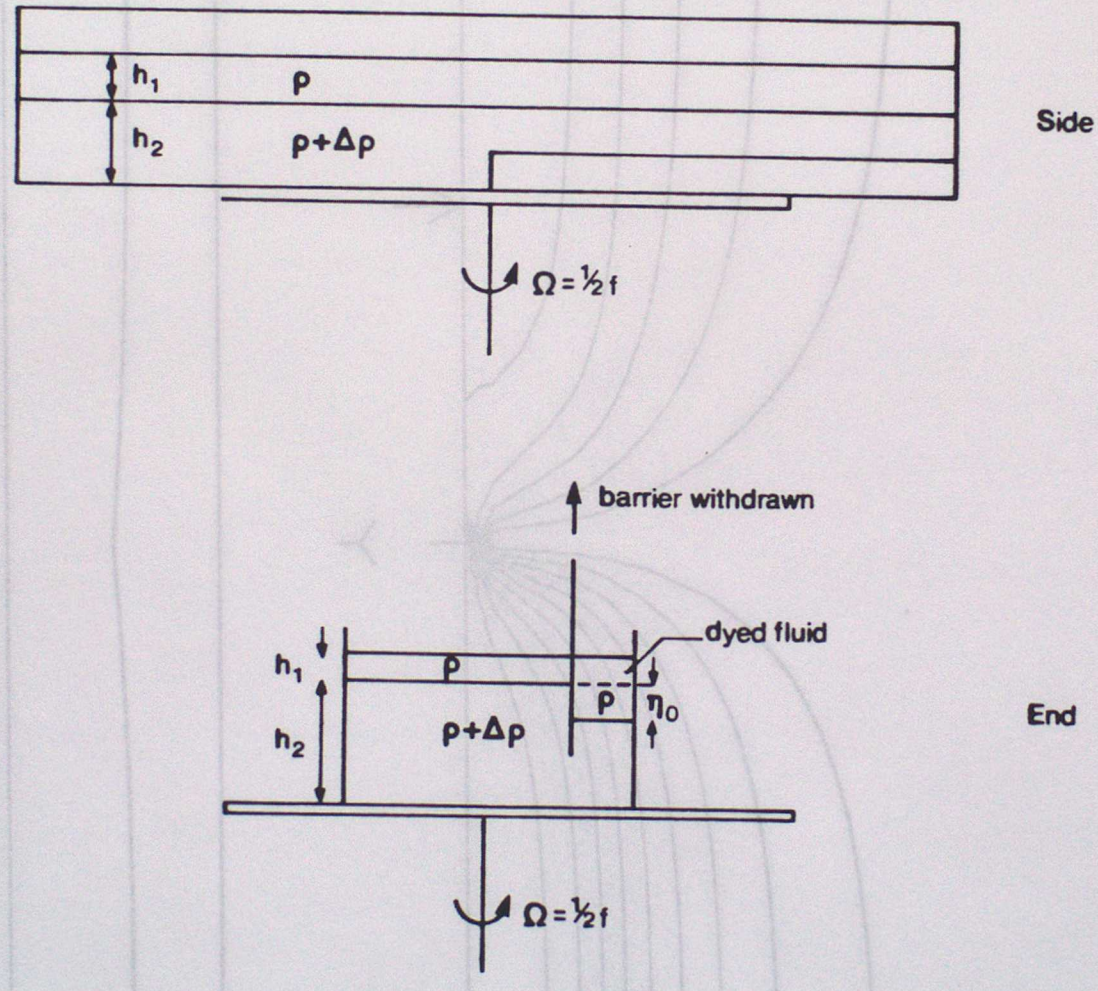
h1
ρ
h2
ρ+Δρ
Side
Ω=½f
barrier withdrawn
dyed fluid
h1
ρ
ρ̄
η0
h2
ρ+Δρ
End
Ω=½f

Fig. 12

Fig 13 a

b

c

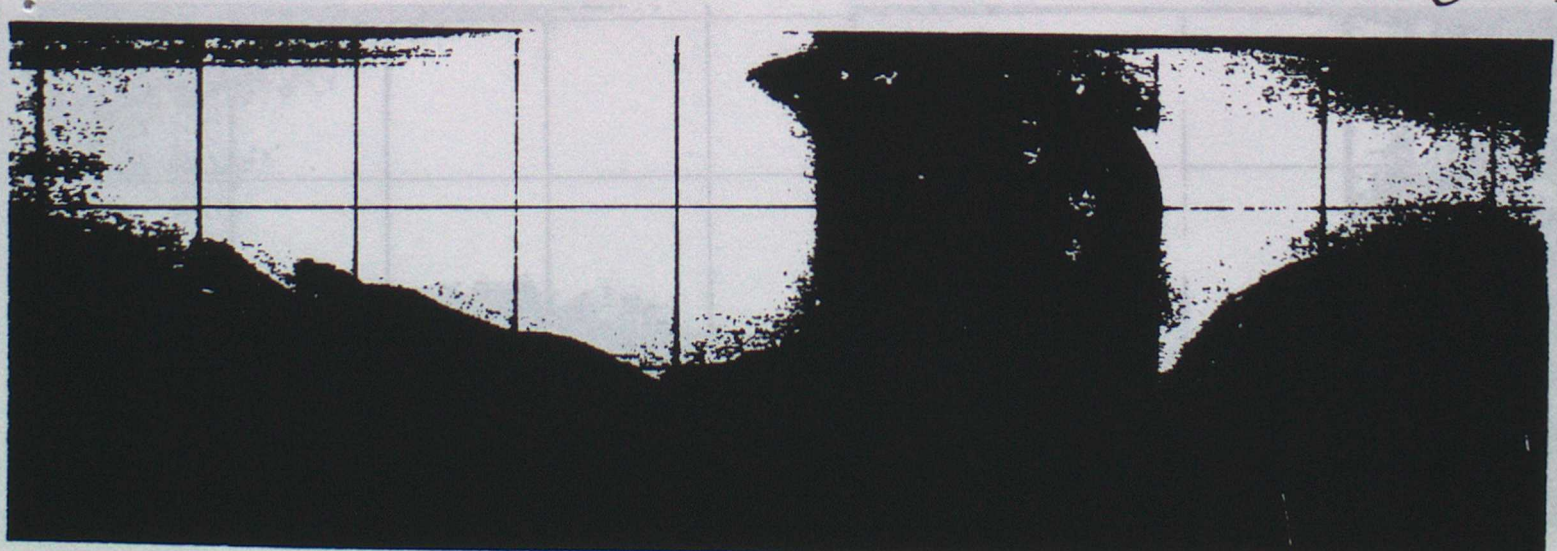

F.g. 14a

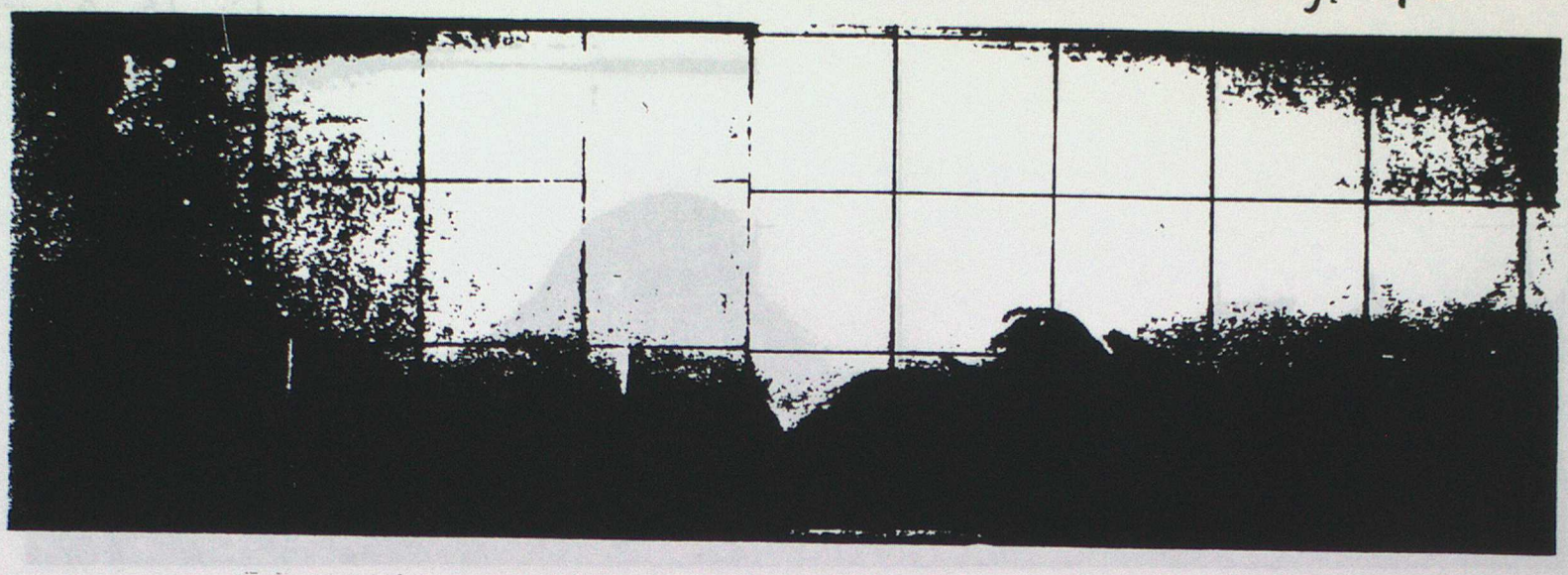

b

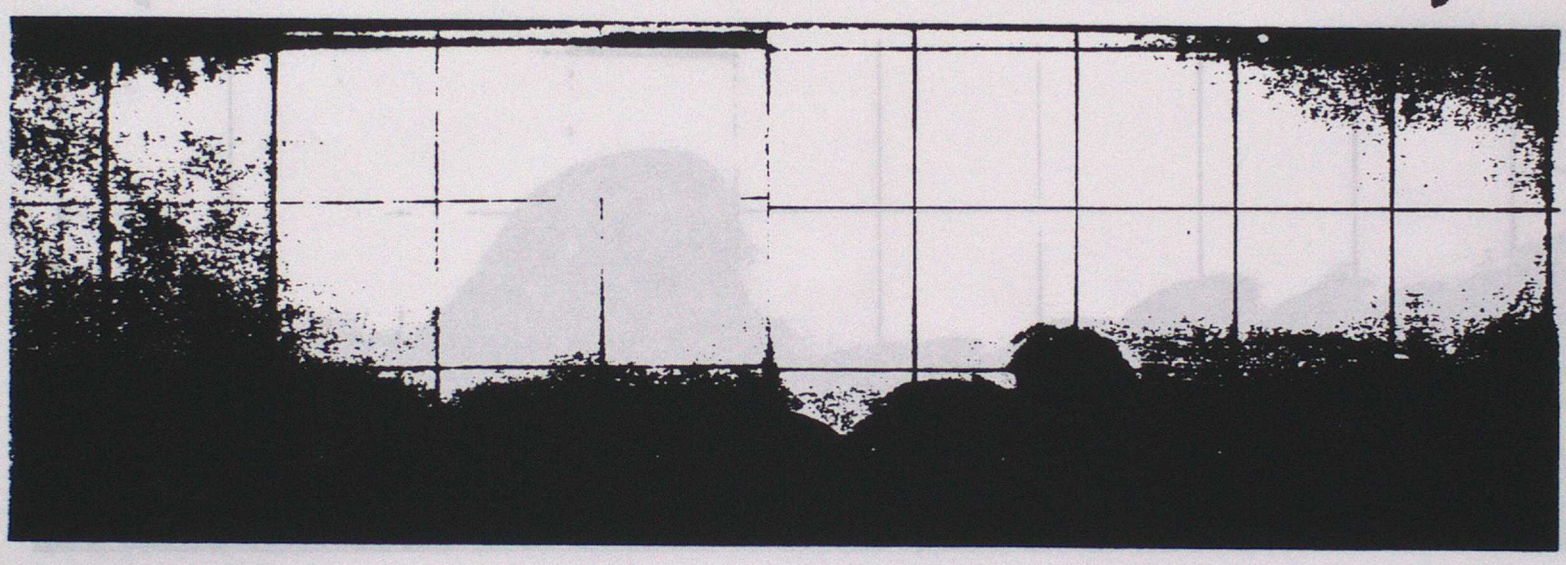

c

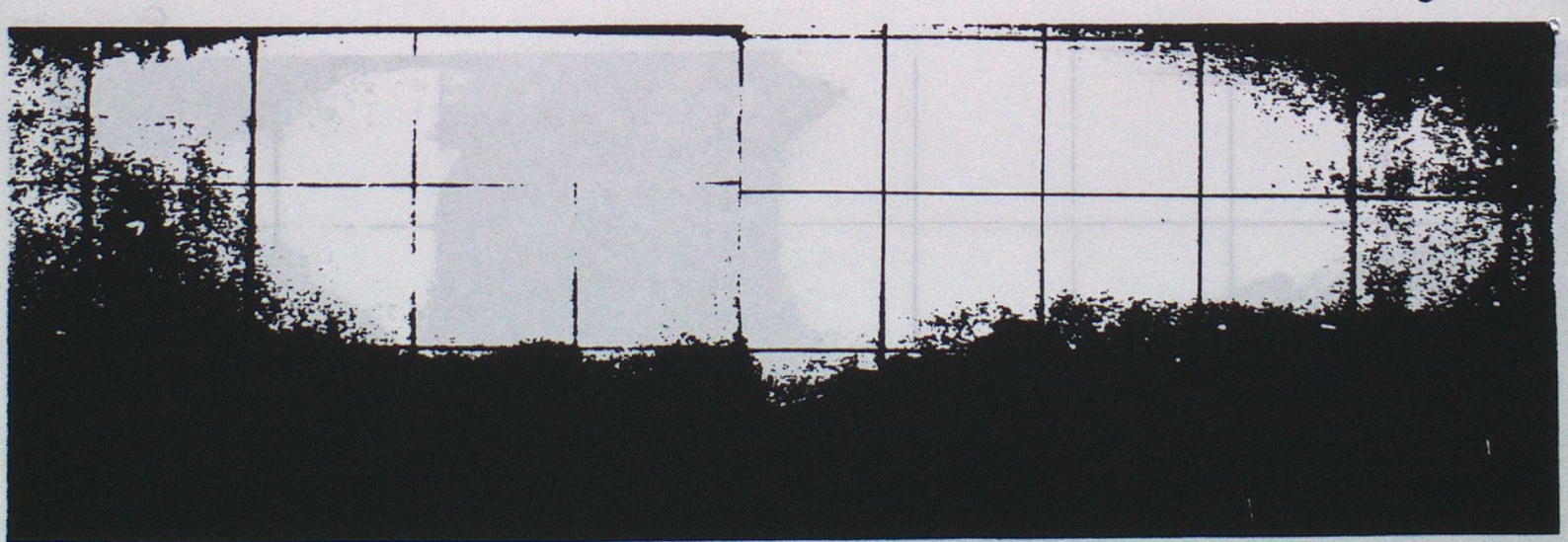

Fig. 15a

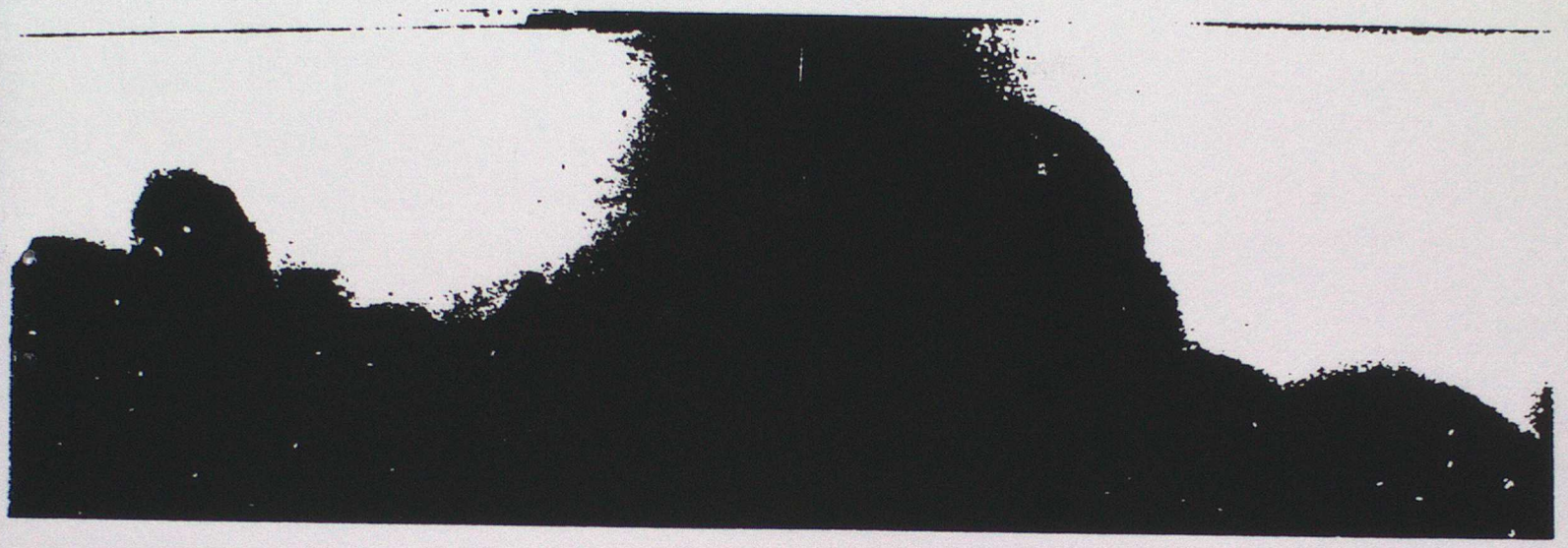

Fig. 15b

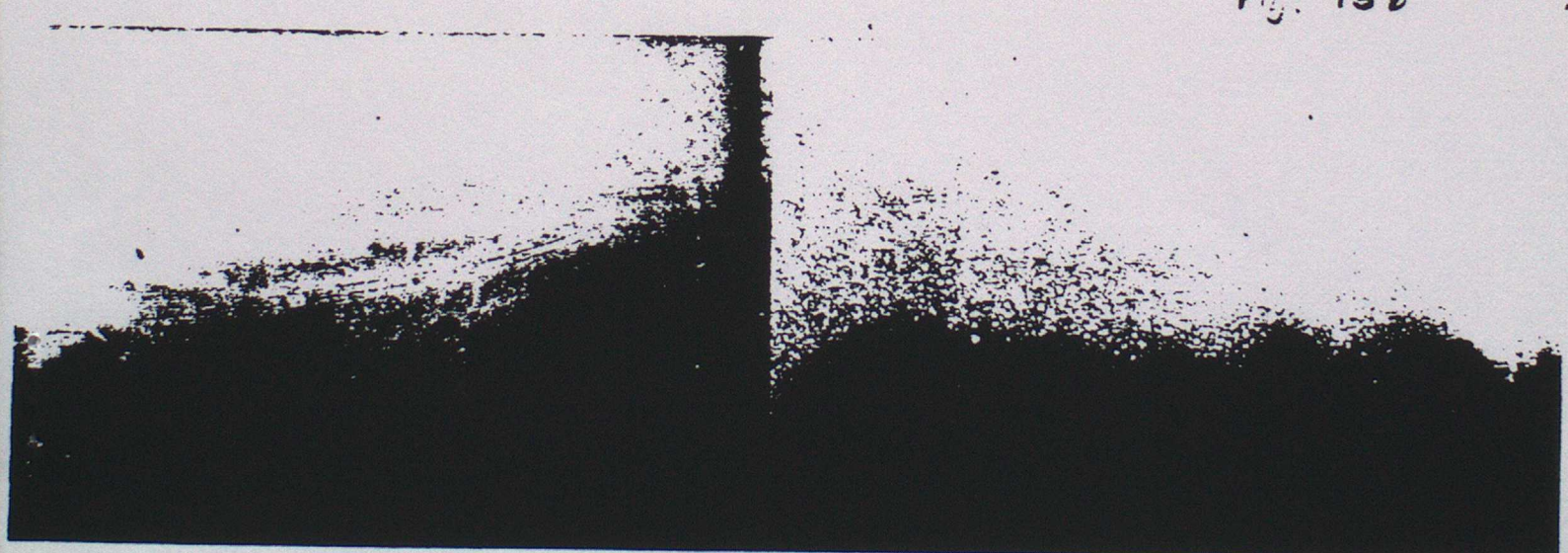

DYNAMICAL CLIMATOLOGY TECHNICAL NOTES

DCTN 1	June 1984	A scheme for incorporating the thermodynamic sea-ice model into a coupled ocean-atmosphere model. C Gordon and M Bottomley
DCTN 2	Sept 1984	The parametrization of the upper ocean mixed layer in coupled ocean/atmosphere models. C Gordon and M Bottomley
DCTN 3	Sept 1984	The response of a simple thermodynamic sea-ice model to GCM forcing appropriate for perennial sea-ice. M Bottomley
DCTN 4	Sept 1984	Potential vorticity in the stratosphere derived using data from satellites. S A Clough, N S Grahame and A O'Neill
DCTN 5	Sept 1984	Simulation of the seasonal cycle of SST using globally specified climatological data to force simple ocean models. N S Grahame
DCTN 6	Sept 1984	Development of an improved GCM radiation scheme. A Slingo and R C Wilderspin
DCTN 7	Sept 1984	On the specification of surface fluxes in coupled atmosphere/ocean general circulation models. J F B Mitchell, C A Wilson and C M Price
DCTN 8	Sept 1984	A survey of possible repercussions of the Soviet river reversal programme on Arctic sea-ice. H Cattle
DCTN 9	Oct 1984	A study of a strong stratospheric warming during January 1982 T D A Fairlie
DCTN 10	Nov 1984	An intercomparison of the Met O 11 N45 model and the Met O 20 11-level model on the Cyber 205 J F Dyson
DCTN 11	Nov 1984	Simulation of observed time series of temperature and precipitation over eastern England. D N Reed
DCTN 12	Nov 1984	Forecasts and analyses of the onset of the Southwest monsoon. R Kershaw
DCTN 13	Nov 1984	On modelling the effects of CO_2 on climate. J F B Mitchell
DCTN 14	Dec 1984	Development of a revised longwave radiation scheme for an atmospheric general circulation model. A Slingo and R C Wilderspin
DCTN 15	Jan 1985	Rossby wavetrains in the stratosphere forced by localised disturbances in the troposphere. C J Marks (Oxford), A O'Neill and V D Pope

DYNAMICAL CLIMATOLOGY TECHNICAL NOTES

DCTN 16	Jan 1985	Observing system experiments using the Meteorological Office's 15-level model. R A Bromley
DCTN 17	Feb 1985	Atmospheric general circulation simulation of the climate of the Mediterranean region. H Cattle
DCTN 18	Feb 1985	Diurnal variation and cloud in a general circulation model. C A Wilson and J F B Mitchell
DCTN 19	Feb 1985	The sensitivity of the Saharan region in a general circulation model. W M Cunnington and P R Rowntree
DCTN 20	Mar 1985	The impact of aircraft observations on analyses and forecasts from the operational 15-level model. B R Barwell
DCTN 21	Mar 1985	Non-linear effects on heat-induced circulation of the tropical atmosphere. A E Gill and P J Phlips
DCTN 22	Apr 1985	Simulation of cloudiness with the U.K. Meteorological Office 11-layer AGCM. A Slingo and R C Wilderspin
DCTN 23	Apr 1985	An integrated approach to the representation of cloud processes. R N B Smith
DCTN 24	May 1985	Nuclear Winter: Calculations of the shortwave radiative effects of soot aerosols. A Slingo and P Goldsmith
DCTN 25	Jul 1985	Sea ice and the Antarctic winter circulation: a numerical experiment. J F B Mitchell and T S Hills
DCTN 26	Jul 1985	A Budyko-Sellers model for study of ocean-atmosphere interaction. W J Ingram
DCTN 27	Aug 1985	The effect of a shoaling thermocline on equatorially-trapped Kelvin waves. A E Gill and B A King
DCTN 28	Sept 1985	CO_2 climate sensitivity and model dependence of results. J F B Mitchell, C A Wilson and W M Cunnington
DCTN 29	Sept 1985	Handbook of the Meteorological Office 11-layer atmospheric general circulation model. Volume 1 : Model Description Edited by A Slingo
DCTN 30	Sept 1985	Impact of land surface variations on African rainfall in general circulation models. P R Rowntree, M F Wilson and A B Sangster

DYNAMICAL CLIMATOLOGY TECHNICAL NOTES

DCTN 31 Nov 1985 The annual cycle of sea level in the eastern tropical Pacific.
G R Bigg and A E Gill

DCTN 32 Nov 1985 An analytic model of the heat-induced tropical circulation in the presence of a mean wind.
P J Phlips and A E Gill

DCTN 33 Nov 1985 The effect of resolution and diffusion on the simulated climate.
J F Dyson